



Published in final edited form as:

*J Pain*. 2022 October ; 23(10): 1629–1645. doi:10.1016/j.jpain.2022.05.009.

## Spinal CCK1 receptors contribute to somatic pain hypersensitivity induced by malocclusion via a reciprocal neuron-glia signaling cascade

Ting Xiang<sup>\*,†</sup>, Jia-Heng Li<sup>\*</sup>, Han-Yu Su<sup>\*</sup>, Kun-Hong Bai<sup>\*</sup>, Shuang Wang<sup>†</sup>, Richard J Traub<sup>‡,2</sup>, Dong-Yuan Cao<sup>\*,1</sup>

<sup>\*</sup>Key Laboratory of Shaanxi Province for Craniofacial Precision Medicine Research, Research Center of Stomatology, Xi'an Jiaotong University College of Stomatology, 98 West 5th Road, Xi'an, Shaanxi 710004, China

<sup>†</sup>Department of Orthodontics, Xi'an Jiaotong University College of Stomatology, 98 West 5th Road, Xi'an, Shaanxi 710004, China

<sup>‡</sup>Department of Neural and Pain Sciences, School of Dentistry; Center to Advance Chronic Pain Research, University of Maryland Baltimore, 650 W Baltimore St, Baltimore, MD 21201, USA

### Abstract

Recent studies have shown that the incidence of chronic primary pain (CPP) including temporomandibular disorders (TMD) and fibromyalgia syndrome (FMS) often exhibit comorbidities. We recently reported that central sensitization and descending facilitation system contributed to the development of somatic pain hypersensitivity induced by orofacial inflammation combined with stress. The purpose of this study was to explore whether TMD caused by unilateral anterior crossbite (UAC) can induce somatic pain hypersensitivity, and whether the cholecystikinin (CCK) receptor-mediated descending facilitation system promotes hypersensitivity through neuron-glia cell cascade signaling. UAC evoked thermal and mechanical pain hypersensitivity of the hind paws from day 5 to 70 that peaked at week 4 post UAC. The expression levels of CCK1 receptors, IL-18 and IL-18 receptors (IL-18R) were significantly up-regulated in the L4-L5 spinal dorsal horn at 4 weeks post UAC. Intrathecal injection of CCK1 and IL-18 receptor antagonists blocked somatic pain hypersensitivity. IL-18 mainly co-localized with microglia, while IL-18R mainly co-localized with astrocytes and to a lesser extent with neurons. These findings indicate that the signaling transduction between neurons and glia at the spinal cord level contributes to the descending pain facilitation through CCK1 receptors during the development of the comorbidity of TMD and FMS.

<sup>1</sup>Address reprint requests to Dong-Yuan Cao, PhD, Key Laboratory of Shaanxi Province for Craniofacial Precision Medicine Research, Xi'an Jiaotong University College of Stomatology, Xi'an, Shaanxi 710004, China. , dongyuan\_cao@hotmail.com. <sup>2</sup>Address reprint requests to Richard J. Traub, PhD, Department of Neural and Pain Sciences, School of Dentistry, University of Maryland Baltimore, Baltimore, MD 21201, USA. , rtraub@umaryland.edu.

**Publisher's Disclaimer:** This is a PDF file of an unedited manuscript that has been accepted for publication. As a service to our customers we are providing this early version of the manuscript. The manuscript will undergo copyediting, typesetting, and review of the resulting proof before it is published in its final form. Please note that during the production process errors may be discovered which could affect the content, and all legal disclaimers that apply to the journal pertain.

The authors state they have no conflict of interest.

## Keywords

Cholecystokinin; IL-18; Temporomandibular disorders; Fibromyalgia syndrome; Comorbidity

---

## 1. Introduction

Pain is an unpleasant sensory and emotional experience associated with actual or potential tissue damage or similar experiences<sup>72</sup>. Chronic primary pain (CPP), such as temporomandibular disorders (TMD) and fibromyalgia syndrome (FMS), has become a serious health problem in clinical practice and has not been satisfactorily resolved due, in part, to an unclear mechanistic understanding<sup>51</sup>. TMD is a common disease of the oral and maxillofacial region. TMD patients often present with masticatory muscle pain, joint pain, and abnormal jaw movement. FMS is a disease with chronic systemic musculoskeletal pain and somatic hyperalgesia. Studies have shown that TMD is often comorbid with FMS, 10%–18.4% of FMS patients have symptoms of TMD, and 71%–94% of TMD patients may suffer from FMS simultaneously<sup>48</sup>. Recently, we found that different modes of stress induced widespread somatic pain hypersensitivity in female rats with orofacial muscle inflammation, establishing a comorbid animal model to investigate the mechanisms of the FMS and TMD<sup>36, 80</sup>. We also reported that cholecystokinin (CCK)-dependent descending facilitation contributed to somatic hypersensitivity in this comorbid pain model<sup>14</sup>.

It has been shown that malocclusion plays an essential role in the development of TMD by leading to an imbalance of the masticatory system and further development of TMD<sup>25, 74, 86, 89</sup>. Thus, the primary purpose of this study was to clarify whether widespread somatic pain hypersensitivity also happens in animals with temporomandibular joint osteoarthritis (TMJ-OA), which is characterized by cartilage loss, subchondral bone sclerosis, osteophyte formation<sup>77</sup>, and increased levels of cytokines, including IL-1 $\beta$  and IL-18<sup>10</sup>. Therefore, we chose a unilateral anterior crossbite (UAC) rat model causing TMJ-OA to explore whether TMD alone can induce the characteristic symptoms of FMS<sup>85</sup>.

Primary sensory afferents from the TMJ project to the trigeminal subnuclei interpolaris/caudalis transition zones (Vi/Vc), and Vi/Vc-rostral ventromedial medulla (RVM) pathway facilitated orofacial hyperalgesia<sup>70</sup>. Therefore, we hypothesized that widespread pain hypersensitivity induced by TMD may be related to the activation of the descending facilitation system. CCK is an important neurotransmitter in the central nervous system (CNS) and can promote pain sensitization by activating a descending facilitatory pathway<sup>24, 43</sup>, thus whether CCK and its receptors in the spinal cord contribute to the widespread pain hypersensitivity induced by UAC was investigated.

Accumulating evidence demonstrates that sustained increases in cytokine and chemokine expression in the CNS promotes chronic widespread pain<sup>27</sup>. Recently, the neuron-glia-neuron signal as the driving force for the occurrence and maintenance of persistent pain has attracted more attention<sup>13, 60, 75</sup>. Inflammatory mediators such as chemokines are released from glial cells<sup>38, 44</sup>. Neuromodulin and chemokines have been widely confirmed as neuron-microglia specific mediators<sup>4, 18</sup>. IL-18, as a closely related family member of IL-1 $\beta$ , is an important regulator of innate and immune response and involved in the process of chronic

pain<sup>17</sup>. IL-18 induces signal transduction by binding to its heterologous complex IL-18  $\alpha/\beta$  receptors. IL-18 receptors (IL-18Rs) are expressed on many cell types, including neurons and glial cells<sup>31, 45</sup>. In the dorsal horn of the spinal cord, IL-18 is uniquely expressed in microglia and its receptors mainly present in astrocytes, and it plays a key role in the development and maintenance of mechanical allodynia<sup>45</sup>. Meanwhile, the early response to peripheral nerve injury in the CNS is mainly the overactive microglia of the spinal cord followed by activation and proliferation of astrocytes<sup>42, 54</sup>. It has been shown that IL-1 $\beta$  upregulates genes which are involved in activation of NF- $\kappa$ B cascade associated with CCK receptor signaling<sup>73</sup>. However, there is no report clarifying the relationship between CCK receptors and IL-18 in the development of pain, and there is no evidence that CCK receptors, IL-18, and glial cell cascade signals in the development of comorbidities of TMD and FMS.

Therefore, the purpose of this study was to establish a TMJ-OA animal model to explore whether it can induce widespread somatic pain hypersensitivity in rats, which is a typical symptom of FMS, and further explore the role of CCK receptors and IL-18-mediated neuron-glia cell signaling cascade in the spinal cord in the TMD-induced somatic pain hypersensitivity.

## 2. Materials and Methods

### 2.1. Animals

Female Sprague-Dawley rats weighing 180–200 g (about 8 weeks of age) were obtained from Xi'an Jiaotong University Laboratory Animal Center (Xi'an, Shaanxi, China) and housed in a climate-controlled room on a 12-hour light/dark cycle (lights on at 7:00 AM). Food and water were available ad libitum. All experiments were approved by the Institutional Animal Care and Use Committees of Xi'an Jiaotong University and the Biomedical Ethics Committee of Xi'an Jiaotong University Health Science Center (approved No. 2019–950), China. The experiments were also adhered to guidelines for experimental pain in animals published by the International Association for the Study of Pain.

### 2.2. UAC rat model

Every rat has two pairs of incisors, and the upper incisor occludes the labial side of the lower incisor ordinarily. UAC surgery was performed on 8-week-old rats according to previous studies<sup>40</sup>. Briefly, after each rat was anesthetized with 2%–3% isoflurane, a section of a metal tube (length, 2.5 mm; inside diameter, 3 mm) was pasted to the left maxillary incisor and a curved section of metal tube (length, 4.5 mm; inside diameter, 3.5 mm) was pasted to the left mandibular incisor. The end of the latter tube was bent to create a 135°-angle leaning toward the labial side to create a cross-bite relationship between the top and bottom incisors (Supplemental Figure 1). Each operation was completed within 3 minutes and all efforts were made to minimize suffering. The tubes were carefully glued with light-curing resin and inspected every day. During the experiment, the metal tubes were not found to drop off. In the sham group, the rats experienced the same procedures without fixing the metal tubes so that the tubes dropped off in a few hours. All animals were fed cylindrical compressed food pellets.

### 2.3. Histological staining and micro-computed tomography (Micro-CT) scanning

UAC and sham operated rats were anesthetized with isoflurane (5%) and sacrificed at 2- and 4-weeks post-UAC. Based on the previous studies, there were no differences in the degenerative changes between the left and right TMJs of UAC rats<sup>76</sup>. Consequently, the left TMJ tissues in each group were used for histological analysis which was hematoxylin and eosin (H&E) staining (n=4), and the right TMJ tissues were fixed in 4% paraformaldehyde for Micro-CT scanning (n = 4).

As the method reported previously<sup>29</sup>, the surface of condylar cartilage was divided equally into the anterior, middle, and posterior portions (Figure 2B). The thickness of hypertrophic layer in each section was measured.

Micro-CT was performed on condyles by the Micro-CT imaging facility (Y. Cheetah, Y-XLON, Germany). The technician performing the scans and analysis was blinded to the treatment groups. One mandible from each experimental group was dissected, cleaned, and fixed in 4% paraformaldehyde. The samples (n = 4 per group) were analyzed by micro-CT. The serial tomographic projections were acquired at 80 kV and 500 mA, with a voxel size of 8  $\mu\text{m}$ , then corrected by the conventional X-rays (0.8  $\mu\text{m}$ ), and constructed three-dimensional images for quantitative evaluation. In order to assess the histomorphometry of the subchondral bone trabeculae, a 0.5 mm  $\times$  0.5 mm  $\times$  0.5 mm cube was selected in the center of the subchondral bone central section of the condyle. Then the ratio of bone volume to tissue volume (BV/TV), trabecular thickness (Tb.Th), trabecular number (Tb.N) and trabecular separation (Tb.Sp) were measured in the subchondral trabecular area.

### 2.4. Behavioral tests

Before and after UAC surgery, the thermal withdrawal latency of hind paws, the mechanical withdrawal threshold of hind paws, upper back and thigh of rats, as well the maxillofacial mechanical threshold were performed. The specific experimental flowchart is shown in Figure 1A.

**2.3.1. Thermal withdrawal latency**—Thermal sensitivity was tested using a plantar thermal test device (Ugo Balile, Gemonio, Italy). Rats were placed in individual plexiglass enclosures on a transparent glass plate and allowed 30 minutes to adapt. The dividers between adjacent rats were non-transparent to reduce mutual interference between rats<sup>23</sup>. After the rat adapted (quiet, no exploratory behavior and grooming behavior), the left hind paw of the rat was stimulated from underneath with infrared radiation. The time from the start to the end of the thermal stimulation was the thermal withdrawal latency. A cut-off of 20 seconds was set to avoid tissue damage. Each rat was measured three times at an interval of 5 minutes, and the average value was taken as the final measurement value.

**2.3.2. Mechanical withdrawal threshold**—The measurement of mechanical withdrawal threshold was a test method to detect the sensitivity of animal paws to mechanical stimuli, which was measured with a series of calibrated von Frey filaments (Stoelting, Wood Dale, IL, USA)<sup>7</sup>. Rats were individually placed in a transparent plexiglass enclosure on a stainless-steel wire grid to adapt for 30 minutes. von Frey filaments

with logarithmically incremental stiffness (0.41–26 g) were used to stimulate the middle plantar part of the right hindpaw perpendicularly. The mechanical withdrawal threshold was determined by gradually increasing and decreasing the intensity of the stimulus (“up and down” method) using the threshold calculation software (JFlashDixon Calculator, University of Arizona, USA). Consistent with the mechanical pain threshold test of the hind paw, we examined the mechanical nociceptive threshold in the other two areas of the body: upper back and thigh. Each filament was placed perpendicularly to the middle upper back at T12 vertebra level and right thigh. A positive stimulus of the thigh was recorded by flinching, lifting or licking of the thigh. Flinching to stimulation of the upper back was considered a positive response.

**2.3.3. Maxillofacial mechanical threshold**—The threshold of maxillofacial masticatory muscle was measured with a series of calibrated von Frey filaments (15–100 g). Rats were constrained in the experimenter’s left hand<sup>6, 59</sup>. They were acclimated to the test environment by normal petting for 2 or 3 days, about half an hour per day, before UAC surgery. The mechanical threshold of bilateral masseter muscles to von Frey’s filaments was measured at fixed time points every day. Stimulation was confined to the masseter muscle area within 1 cm of the left maxillofacial region from the midpoint of the connection between the outer canthus and the ear canal. A rapid “head shrinking” appearance or “calling” response is considered a positive reaction to the stimulation<sup>19</sup>. Consistent with the mechanical pain threshold test of the hind paw, the “up and down” method was used.

#### 2.4. Intrathecal injection

Rats were anesthetized with 2%–3% isoflurane, the hair on the low back was shaved, and the operation area was disinfected. The rat was placed in a prone position to bend the lumbosacral vertebrae with a round tube underneath the abdomen. A 25-gauge stainless steel needle attached to a glass microsyringe was inserted into the intervertebral space between the L4-L5 vertebrae. A quick flick of the tail indicated that the needle entered into the intrathecal space. IL-18 binding protein (IL-18BP, 1 µg) diluted in phosphate buffered saline (PBS) or CCK1 receptor antagonist loxiglumide (100 nmol) diluted in saline was intrathecally injected (i.t.; 10 µL) for 5 consecutive days at 4 weeks post UAC establishment. The vehicle group was injected with equal volume of saline or PBS. The doses of drugs were decided based on previous studies<sup>38, 82</sup> and our preliminary studies. The specific experimental flowchart is shown in Figures 1B and 1C.

#### 2.5. Western blot

Rats were anesthetized with isoflurane (5%) and quickly decapitated at 2 and 4 weeks after UAC surgery. The spinal cord was flushed out with ice-cold saline<sup>5</sup>. The lumbar spinal segments (L4-L5) were collected, and the dorsal part of spinal cord was isolated and stored at – 80 °C until use. Tissues were lysed in RIPA lysis buffer in a mixture of phosphatase inhibitors and protease inhibitors and centrifuged at 10,000 rpm for 10 minutes at 4°C. The supernatant was collected and the bicinchoninic acid (BCA) method was used to determine the protein concentration. The protein sample (18 µg) was separated on 4–12% SDS-PAGE and blotted onto PVDF membrane after denaturation, which was blocked in blocking buffer for 2 hours, and then incubated with primary antibodies for

CCK1 receptor (1:1000, Bioss, bs-11514R, Beijing, China), CCK2 receptor (1:1000, Bioss, bs-1777R), IL-18 (1:1000, Proteintech, 10663-1-AP, Wuhan, China), IL-18R (1:500, Santa Cruz Biotechnology, sc-80051, Dallas, TX, USA) and GAPDH (1:4000, Boster, BA2913, Wuhan, China) overnight at 4°C. After washing, the membranes were incubated with HRP-conjugated secondary anti-bodies (1:5000) for 2 hours at room temperature. An enhanced chemiluminescence (ECL) detection system (Thermo Scientific, Waltham, MA, USA) was used for positive immunoreaction detection. Image J software was used to analyze the density of immunoreactive bands.

## 2.6. Immunohistochemistry

Four weeks after the UAC model was established, the rats were deeply anesthetized with isoflurane (5%), and transcardially perfused with 250 mL of cold saline (4°C) followed by 500 mL of 4% paraformaldehyde. The L4-L5 spinal segments were removed, and post-fixed in paraformaldehyde for 24 hours. Then the spinal cord was immersed in 30% sucrose until the spinal cord sank. Paraffin sections (10 µm) were obtained using a microtome and every six sections were collected in 0.1 M PBS. For immunofluorescence staining, depending on the type of secondary antibody host, the free-floating slices were blocked with TBS containing 10% goat serum for 2 hours, and incubated in the primary antibody overnight at 4°C. The sections were washed in 0.05 M Tris-HCl (pH 7.4; 3 times, 5 minutes each), and then incubated in the secondary antibody for 2 hours at room temperature and washed. Sections were mounted on slides and covered with glycerin for observation using a confocal microscope (Pannoramic DESK, P-MIDI, P250, 3D HISTECH, Hungary). The dilution of antibodies used included anti-IL-18 (1:50, Proteintech, 10663-1-AP), anti-IL-18R (1:200, Bioss, bs-2615R), anti-NeuN (1:5000, Servicebio, GB13138, Wuhan, China), anti-gial fibrillary acidic proteins (anti-GFAP, 1:8000, Servicebio, GB12096), and anti-Iba-1 (1:5000, Servicebio, GB131051). Double immunofluorescence showed higher-magnification photographs in the superficial dorsal horn (layer I-III). To determine the localization of IL-18/IL-18R with neurons and glia cells, we examined the colocalization between IL-18/IL-18R and several biochemical markers. Specifically, six sections per rat were selected randomly for each group, and 6–8 visual fields per section were captured. The images of the superficial dorsal horn (layer I-III) of the spinal cord were captured under the objective lens of ×20.

## 2.7. Drugs

Loxiglumide (MedChemExpress, 107097-80-3, USA) was dissolved in saline and L-18BP (R&D systems, 119-BP-100, Abingdon, UK) was dissolved in PBS. Saline and PBS have no consequential effect on spinal cord nociceptive information transmission<sup>26</sup>.

## 2.8. Data analysis

All data are presented as mean ± SEM. Statistical and figure analyses were performed using GraphPad Prism 8 software. The *t*-test analysis was used to compare the data of CCK1, CCK2, IL-18 and IL-18R expression in the L4-L5 spinal dorsal horn, as well as the quantitative results of Micro-CT between the experimental groups. Two-way ANOVA was used to compare the data of the thermal withdrawal latency, mechanical withdrawal

threshold, maxillofacial mechanical threshold and thickness of hypertrophic layer between the sham and UAC groups at different time points.  $p < 0.05$  was considered significant.

### 3. Results

#### 3.1. Establishment of TMJ-OA animal model

**3.1.1. Histological changes**—In the sham group, the condyle cartilage showed normal tissue structure. Specifically, condyle cartilage includes four layers, namely the fibrous layer, the proliferative layer, the hypertrophic layer and the endochondral ossification layer (Figure 2A). However, at 2 and 4 weeks post UAC, OA-like lesions were observed, which were characterized by reduced number and size of chondrocytes in cartilage, irregular cell arrangement, nuclear pyknosis, and even cell-free areas. The thickness of the hypertrophic layer at 4 weeks post UAC was lower than that in the age-matched sham group (Figure 2C). To compare cartilage thickness changes in different portions, the thickness of the hypertrophic layer in each portion was determined (Figure 2B). The thickness of the hypertrophic layer in the middle portion at 2 and 4 weeks post UAC establishment was significantly lower than that of the sham group at the same time point (t-test: 2 weeks:  $p = 0.0059$ ; 4 weeks:  $p = 0.0470$ , Figure 2C, E). The hypertrophic layer at the anterior portion in the UAC group was significantly reduced at 4 weeks (2 weeks:  $p = 0.1257$ ; 4 weeks:  $p = 0.0345$ , Figure 2D). However, the hypertrophic layer at the posterior portion of the UAC group was similar to the sham group at 2 and 4 weeks post UAC (2 weeks:  $p = 0.1378$ ; 4 weeks:  $p = 0.9425$ , Figure 2 F).

**3.1.2. Morphological parameters of bone tissue**—Micro-CT reflects the changes in the subchondral bone morphology of the condyle in three dimensions, which is a quantitative indicator of bone structure and bone density (Figure 3A). According to the micro-CT images, the UAC group showed significant loss of subchondral trabecular bone at 4 weeks post UAC, which was characterized by an increase in trabecular bone separation (Tb. Sp,  $p = 0.0035$  vs. the sham group, Figure 3B) and a decrease in the bone volume fraction (bone volume/tissue volume, BV/TV,  $p = 0.0008$  vs. the sham group, Figure 3C). The Tb.Sp ( $p = 0.4842$ ) did not change significantly, but the BV/TV significantly decreased ( $p = 0.0027$ ) at 2 weeks post UAC vs. the sham group. There were no differences in the trabecular thickness (Tb. Th, Figure 3D) and the number of trabeculae (Tb. N, Figure 3E) at 2 weeks ( $p = 0.6383$  and  $0.9311$ , respectively) and 4 weeks ( $p = 0.9573$  and  $0.3975$ , respectively) post UAC compared with the sham group.

**2.2 3.2. UAC induces maxillofacial pain sensitization, thermal hyperalgesia in hind paw and mechanical allodynia in hind paw, upper back and thigh:**

All rats were healthy, but there was a decrease in body weight in the UAC group compared to sham rats (two-way ANOVA,  $F_{13,238} = 0.5244$ ,  $p = 0.9084$  for interaction;  $F_{1,238} = 25.58$ ,  $p < 0.0001$  for time factor;  $F_{13,238} = 14.24$ ,  $p < 0.0001$  for group factor, Supplemental Figure 2). UAC reduced maxillofacial mechanical pain threshold, thermal withdrawal latency and mechanical withdrawal threshold in the hind paws, upper back and thigh of rats compared to baseline. There were no statistical differences between the UAC group and the sham group at the baseline level. On the first day after the UAC was established, the maxillofacial

mechanical threshold decreased significantly, which was most obvious on the 4th day post UAC, then it gradually blocked on the 8th and 12th days post UAC (left masseter: two-way ANOVA,  $F_{13,102} = 2.596$ ,  $p = 0.0038$  for interaction;  $F_{1,10} = 7.946$ ,  $p = 0.0182$  for time factor;  $F_{13,130} = 3.184$ ,  $p = 0.0004$  for group factor, Figure 4A; right masseter: two-way ANOVA,  $F_{13,102} = 2.108$ ,  $p = 0.0196$  for interaction;  $F_{1,10} = 8.430$ ,  $p = 0.0157$  for time factor;  $F_{13,130} = 2.511$ ,  $p = 0.0042$  for group factor, Figure 4B). There was no difference in the maxillofacial mechanical threshold between the left and right masticatory muscles (UAC: two-way ANOVA,  $F_{13,130} = 0.3555$ ,  $p = 0.9806$  for interaction;  $F_{1,10} = 0.1020$ ,  $p = 0.7560$  for time factor;  $F_{13,130} = 6.603$ ,  $p < 0.0001$  for group factor, Figure 4C; sham: two-way ANOVA,  $F_{13,104} = 1.156$ ,  $p = 0.3222$  for interaction;  $F_{1,8} = 1.740$ ,  $p = 0.2236$  for time factor;  $F_{13,104} = 1.029$ ,  $p = 0.4297$  for group factor, Figure 4D).

Following UAC thermal and mechanical sensitivity increased in the hind paws. The thermal withdrawal latency of the hind paws was significantly decreased in the UAC group compared to sham (two-way ANOVA,  $F_{9,70} = 2.955$ ,  $p = 0.0049$  for interaction;  $F_{1,10} = 85.69$ ,  $p < 0.0001$  for time factor;  $F_{9,90} = 8.348$ ,  $p < 0.0001$  for group factor, Figure 5A). Likewise, the mechanical withdrawal threshold of the hind paws in the UAC group was significantly lower compared with the sham group (two-way ANOVA,  $F_{9,70} = 3.322$ ,  $p = 0.020$  for interaction;  $F_{1,10} = 8.316$ ,  $p = 0.0163$  for time factor;  $F_{9,90} = 2.958$ ,  $p = 0.0040$  for group factor, Figure 5B). In order to further confirm the somatic pain hypersensitivity induced by UAC, in a separated group we examined the mechanical nociceptive threshold in other two areas of the body: upper back and thigh of rats. There were significant differences among groups in the mechanical withdrawal threshold in the upper back (two-way ANOVA,  $F_{9,180} = 2.559$ ,  $p = 0.0086$  for interaction;  $F_{1,180} = 61.48$ ,  $p < 0.0001$  for time factor;  $F_{9,180} = 2.631$ ,  $p = 0.0070$  for group factor, Figure 5C) and the thigh of rats (two-way ANOVA,  $F_{9,180} = 3.998$ ,  $p = 0.0001$  for interaction;  $F_{1,180} = 161.1$ ,  $p < 0.0001$  for time factor;  $F_{9,180} = 4.203$ ,  $p < 0.0001$  for group factor, Figure 5D). In the sham group there was no effect in the thermal withdrawal latency or mechanical withdrawal threshold compared to baseline. Taken together, these findings indicate that UAC induces widespread somatic pain hypersensitivity, a typical characteristic observed in patients with FMS.

### 3.3. CCK1 receptors are involved in the somatic pain hypersensitivity induced by UAC

CCK is a neuropeptide with abundant content and wide distribution in the CNS. It has been shown that CCK can promote pain sensitization by activating descending facilitation from the PAG and RVM<sup>43</sup>. To explore whether spinal CCK receptors contribute to UAC-induced widespread pain hypersensitivity in the hind paws, we investigated the protein expression of CCK receptors in the L4-L5 spinal dorsal horn, the site of spinal nociceptive signal processing related to the hind limbs. The Western blot data showed that the expression of CCK1 receptors significantly increased in the UAC group compared with the sham group at 4 weeks, but not 2 weeks, post UAC ( $p = 0.0497$  at 4 weeks,  $p = 0.1307$  at 2 weeks, Figure 6A, B). There were no significant differences in the expression of CCK2 receptors between those two groups ( $p = 0.4642$  at 4 weeks,  $p = 0.5390$  at 2 weeks, Figure 6A, B), suggesting that CCK1 receptors, but not CCK2 receptors, in the spinal cord were up-regulated in the UAC rats.



To confirm whether the increased CCK1 receptors contribute to UAC-induced widespread pain hypersensitivity in female rats, the CCK1 receptor antagonist loxiglumide was intrathecally injected at 4 weeks post UAC. Compared with the saline treated group, loxiglumide blocked the reduction of thermal withdrawal latency (two-way ANOVA,  $F_{10,165} = 1.975$ ,  $p = 0.0390$  for interaction;  $F_{1,165} = 94.39$ ,  $p < 0.0001$  for time factor;  $F_{10,165} = 3.831$ ,  $p = 0.0001$  for group factor, Figure 6C) and mechanical withdrawal threshold (two-way ANOVA,  $F_{10,160} = 2.516$ ,  $p = 0.0077$  for interaction;  $F_{1,16} = 11.78$ ,  $p = 0.0034$  for time factor;  $F_{10,160} = 1.221$ ,  $p = 0.0281$  for group factor, Figure 6D) in the UAC group. These results indicate that the up-regulation of CCK1 receptors in the spinal cord play a critical role in UAC-induced widespread pain hypersensitivity. To further evaluate the effects of CCK1 receptor antagonist on the sham-operated animals, loxiglumide was administered to sham treated rats and tested for thermal and mechanical hyperalgesia. The data showed that loxiglumide did not change the pain thresholds in sham rats (Supplemental Figure 3).

### 3.4. Up-regulated IL-18 in microglia and IL-18 receptors in astrocytes mediate microglia-astrocytic interaction during UAC-induced widespread pain hypersensitivity

Recently, IL-18-mediated signaling pathways have been extensively studied in the occurrence and development of chronic pain by regulating the interaction of microglia and astrocytes<sup>38, 45, 57, 83</sup>. It has been shown that IL-18 is mainly expressed in microglia in different animal pain models. Therefore, in order to explore the role of IL-18 in UAC-induced widespread pain hypersensitivity, we examined the expression of IL-18 and IL-18R in the spinal cord. Western blot analysis showed that the expression levels of IL-18 and IL-18R in the spinal cord significantly increased at 4 weeks post UAC compared with the sham group (IL-18:  $p = 0.0403$ ; IL-18R:  $p = 0.0341$ ; Figure 7A), but there were no significant differences in the expression of IL-18 and IL-18R at 2 weeks post UAC (IL-18:  $p = 0.2027$ ; IL-18R:  $p = 0.1727$ ; Figure 7B). Biochemical markers for neurons (NeuN), microglia (Iba-1) and astrocytes (GFAP) were used to determine the expression locations of IL-18 and IL-18R using immunohistochemistry. Double immunostaining further confirmed that IL-18 was mainly expressed in microglia in the dorsal horn (Figure 8A), which was consistent with previous observations<sup>38</sup>. IL-18 had little and no colocalization with GFAP and NeuN (Figure 8B, C), respectively. However, in contrast to IL-18 expression in microglia, IL-18R was mainly expressed in astrocytes and a lesser extent in neurons (Figure 9A, B), but not in microglia (Figure 9C).

In order to further determine the role of IL-18 in somatic pain hypersensitivity induced by UAC, IL-18-binding protein (IL-18BP), which functions as an IL-18 antagonist by binding to IL-18R and blocking its biological activity, was intrathecally injected for 5 consecutive days at 4 weeks post UAC. IL-18BP significantly blocked the decrease in the thermal withdrawal latency (two-way ANOVA,  $F_{9,60} = 3.262$ ,  $p = 0.0027$  for interaction;  $F_{1,60} = 17.78$ ,  $p < 0.0001$  for time factor;  $F_{9,80} = 4.297$ ,  $p = 0.0001$  for group factor, Figure 10A) and mechanical withdrawal threshold (two-way ANOVA,  $F_{9,150} = 1.139$ ,  $p = 0.3392$  for interaction;  $F_{1,150} = 15.26$ ,  $p = 0.0001$  for time factor;  $F_{9,150} = 2.019$ ,  $p = 0.0408$  for group factor, Figure 10B). The behavioral results combined with the Western blot data indicate that IL-18 activation in the spinal cord contributes to somatic pain hypersensitivity induced by UAC.

### 3.5. Spinal CCK1 receptors are involved in the activation of IL-18 and its receptors, leading to UAC-induced somatic pain hypersensitivity

It has been shown that IL-1 $\beta$  can up-regulate CCK receptor signaling and participate in the activation of the NF- $\kappa$ B cascade related to CCK receptor signaling<sup>71, 73</sup>. These effects are thought to be related to pain sensitization<sup>66</sup>. Therefore, we tested the relationship between CCK1 receptors and IL-18 in the spinal cord. Western blot data showed that intrathecal injection of CCK1 receptor antagonist loxiglumide for 5 consecutive days significantly reduced the expression of IL-18 ( $p = 0.0483$ , Figure 11A) and IL-18R ( $p = 0.0336$ , Figure 11B) in the spinal dorsal horn at 4 weeks post UAC establishment compared with the saline group. Therefore, the release of IL-18 and the activation of IL-18R on glial cells in the spinal cord may be involved in the CCK-dependent descending facilitation post UAC establishment.

## 4. Discussion

In the present study we demonstrated that UAC induced long-term somatic pain hypersensitivity, establishing a new animal model of TMD and FMS comorbidity. We report that spinal CCK1 and IL-18 receptors are involved in central sensitization in the development of comorbid pain. In addition, our findings demonstrate that a neuron-glia signaling cascade is involved in the mechanisms underlying spinal CCK1 receptor-mediated hypersensitivity.

In the past few decades, CPPs such as FMS<sup>2</sup> and TMD<sup>33</sup> have been increasingly viewed as a serious health problem in clinical practice and comorbidity of these diseases frequently occur. However, the mechanism underlying this comorbidity is unclear, leading to unsatisfactory treatment outcomes. Therefore, it is essential to investigate coexisting mechanisms of comorbid pain and develop targeted drugs to effectively prevent and treat these pain syndromes.

Central sensitization underlies chronic pain conditions, including OA and FMS<sup>20, 68</sup>. In general, central sensitization is an adaptive process that reverts back to normal after nociceptive afferent input has ceased. However, persistent, intense noxious stimuli can lead to persistent central sensitization<sup>69</sup>. It has been reported that OA patients experience decreased pain sensitivity following successful arthroplasty<sup>21, 32</sup>, suggesting that the dependence of central sensitization and pain on peripheral tissue impulse input in these patients. Recently, a few studies have reported the impact of occlusion on maxillofacial tissues, and the possible impact of malocclusion on the CNS has gained much attention<sup>6, 30</sup>. In the previous study, Wang et al. found that at the 2 and 4 weeks after UAC was established, OA-like lesions were observed in the cartilage, becoming more severe over time<sup>76</sup>. Our data show that UAC caused a long-term, recoverable decrease in maxillofacial mechanical threshold, which occurred before the widespread somatic pain hypersensitivity. Therefore, we propose that UAC acts as an injury stimulus in the maxillofacial area that is signaled into the trigeminal-subnuclei caudalis (Vc) further triggering persistent central sensitization in the brain areas and activates descending pathways that facilitate pain processing<sup>1, 9, 46</sup>.

Stress caused by the malocclusion itself and alterations in feeding might contribute to the widespread pain hypersensitivity. In a previous study, Liu et al.<sup>41</sup> found that UAC, as an unpleasant external stimulus, generated anxiety-like behavior 2 weeks after surgery. As the main component of the descending pain modulatory system, the midbrain periaqueductal gray matter (PAG)<sup>47</sup> and the rostral ventromedial medulla (RVM)<sup>39</sup> regulate nociceptive transmission and processing in the spinal dorsal horn<sup>8</sup>. The findings indicate that central sensitization underlying the development of pain hypersensitivity depends on peripheral nerve injury increasing afferent drive activating a descending facilitation arising from the RVM that likely requires the maintenance of descending CCK receptor-mediated facilitation in the spinal cord<sup>55</sup>.

CCK signaling is part of the descending facilitation system<sup>24</sup>, which drives the development of pain hypersensitivity<sup>43, 62</sup>. Some studies have shown that CCK located in the PAG, RVM, and spinal cord plays a pro-nociceptive role in pain modulation<sup>55, 81</sup>. For example, the RVM promotes the activation of CCK in the spinal cord<sup>55</sup>. CCK acts through CCK1 and CCK2 receptors, both of which are coupled to the Gq/PLC/DAG signaling pathway, which induces calcium efflux from intracellular storage<sup>15, 34, 35</sup>. Under stress stimulation, ON-cells in the RVM can be directly activated by CCK2 receptors promoting pain sensitization, while inhibiting the activity of CCK2 receptors in the RVM can effectively reverse the pain hypersensitivity caused by chronic stress<sup>28, 43, 62</sup>. Studies have reported that CCK1 receptors are expressed by both viscer- and somato-sensory primary sensory neurons, acting as a mediator in sensory processing at the spinal level<sup>3</sup>. Therefore, we propose that CCK receptors are closely related to the widespread somatic pain hypersensitivity induced by UAC. In a previous study, we confirmed that CCK2 receptors-dependent descending pain modulation at the spinal level was involved in somatic pain hypersensitivity induced by orofacial inflammatory pain combined with stress<sup>14</sup>. However, the mechanism by which these events are sequentially activated through neuron-astrocytic interactions is novel and unpredicted. Interestingly, we noticed that the expression of CCK1 receptors, but not CCK2 receptors, significantly increased in the L4-L5 spinal dorsal horn at 4 weeks post UAC and the blockade of spinal CCK1 receptors totally blocked UAC-induced thermal hyperalgesia and mechanical allodynia in the hind paws. A recent study showed that CCK-positive neurons distributed in layers III-IV of the spinal dorsal horn highly overlap with protein kinase C $\gamma$ -positive neurons at the layers II/III border, playing an important role in mechanical allodynia<sup>56</sup>. Some studies showed that CCK2 receptors, but not CCK1 receptors, play a major role in pain perception, opioid dependence and other processes<sup>78, 87</sup>. Multiple studies have found that CCK1 and CCK2 have opposite effects on behavior actions<sup>22, 37, 58</sup>. Therefore, the various subtypes of CCK receptors and their different sensitivity levels are not consistent, determining the diversity of CCK's biological functions. Our present data (Figure 6) may give us a clue that this phenomenon is related to the different functions of CCK1 and CCK2 receptors. These findings suggest that UAC-induced widespread somatic pain hypersensitivity is maintained by neurons in the spinal cord which are sensitive to CCK via CCK1, but not CCK2 receptors.

It has been shown that the central pain mechanism of FMS in the induction and maintenance of chronic pain not only relies on neuronal activation, but also glial activation<sup>67</sup>. Although spinal glial hyperactivity has been reported in studies of TMD and FMS<sup>79, 88</sup>, few studies

investigated the involvement of spinal CCK receptors in spinal glial hyperactivity, as well as the function of IL-18, especially in the pain model of TMD and FMS comorbidity. In the dorsal horn of the spinal cord, the unique expression of IL-18 in microglia and its receptors mainly presenting in astrocytes plays a key role in the development and maintenance of mechanical allodynia<sup>45</sup>. The present study showed that UAC caused a significant increase in the expression of IL-18 and IL-18R in the spinal dorsal horn at 4 weeks post UAC. However, IL-18BP only temporarily relieved the somatic pain hypersensitivity compared with the analgesic effect of CCK1 receptor antagonists (Figure 10). The reason may be that IL-18BP as a secreted glycoprotein cannot be anchored to the cell membrane due to the lack of a transmembrane domain<sup>12</sup>.

In the present study intrathecal injection of a CCK1 receptor antagonist lowered IL-18 expression levels in the spinal dorsal horn, implying that IL-18 may be one of the important cytokines activated by CCK1 receptors and subsequently participates in the development of somatic pain sensitization. Double immunostaining verified that IL-18 in the spinal cord was mainly co-expressed with microglia, and IL-18R was mainly co-expressed with astrocytes, but not in microglia and neurons. Therefore, how CCK neurons produce IL-18 by activating microglia, and then bound to IL-18 receptors on astrocytes to participate in the occurrence of somatic hyperalgesia aroused our interest. A few studies focused on the neuron-glia cell-neuron interaction as the driving force to induce and maintain the pain process<sup>18, 64, 75, 88</sup>. Microglial cells in the spinal cord have an established role in sensitization of pain processing<sup>13</sup>. Under normal and pathological conditions, glial cells in the spinal cord act as immune effector cells and play a key role in promoting persistent pain states<sup>13, 16, 50, 65, 84</sup>. When microglia and astrocytes in the spinal cord are activated, they synthesize and release factors that promote neuronal excitability and nociceptive transmission<sup>11, 52, 63</sup>, thus contributing to the occurrence and development of pain. Guo et al.<sup>18</sup> found that 5-HT<sub>3</sub> receptor-expressing neurons in the spinal cord induced chemokine production, activated microglia to release IL-18 and bind to IL-18R on astrocytes. Then the combination further phosphorylated N-methyl-D-aspartic acid (NMDA) receptors in the spinal cord and ultimately led to hyperalgesia. In animal models of bone cancer pain, IL-18 in the spinal cord regulates NMDA receptor phosphorylation by binding to IL-18R<sup>38</sup>. Furthermore, IL-18 signal activation may lead to the secretion of a variety of cytokines, including TNF- $\alpha$  and IL-1 $\beta$ . The involvement of IL-18R/NF- $\kappa$ B signaling pathway in astrocytes in hyperalgesia has also been confirmed. IL-18 binds to the ligand receptor IL-18R $\alpha$ , recruiting the co-receptor IL-18R $\beta$  to form a high-affinity complex, which activates downstream signals. IL-18 triggers the intracellular signal cascade and induces the dependent expression of NF- $\kappa$ B and AP-1 pro-inflammatory cytokines, chemokines, and secondary mediators of the inflammatory response<sup>57, 61</sup>.

Overall, our current study suggests that active CCK1 receptor-dependent descending facilitation after TMD may mediate central mechanisms underlying the development of widespread somatic pain in our comorbid pain model via a reciprocal neuron-glia signaling cascade.

## 5. Conclusion

In conclusion, activation of CCK1 receptors in the spinal cord contributes to widespread somatic pain hypersensitivity induced by TMD. The activation of glial cells in the spinal cord promotes the release of IL-18 to further mediate this pain hypersensitivity. Neuron and glial cell cascade signals play an important role in the development of the somatic pain hypersensitivity. These results provide novel therapeutic targets for the clinical treatment of TMD and FMS comorbidities.

## Supplementary Material

Refer to Web version on PubMed Central for supplementary material.

## Disclosures :

This work was supported by the National Natural Science Foundation of China (81971049, 81671097), the Social Development Program of Shaanxi Province, China (2020SF-018) to DYK, and the National Institutes of Health, USA (R01 DE029074) to RJT.

## References

1. Baron R, Hans G, Dickenson AH. Peripheral input and its importance for central sensitization. *Ann Neurol*. 74:630–636, 2013 [PubMed: 24018757]
2. Bhargava J, Hurley JA: Fibromyalgia. In: StatPearls, Treasure Island (FL), 2021.
3. Broberger C, Holmberg K, Shi TJ, Dockray G, Hokfelt T. Expression and regulation of cholecystokinin and cholecystokinin receptors in rat nodose and dorsal root ganglia. *Brain Res*. 903:128–140, 2001 [PubMed: 11382396]
4. Calvo M, Zhu N, Tsantoulas C, Ma ZZ, Grist J, Loeb JA, Bennett DLH. Neuregulin-ErbB Signaling Promotes Microglial Proliferation and Chemotaxis Contributing to Microgliosis and Pain after Peripheral Nerve Injury. *J Neurosci*. 30:5437–5450, 2010 [PubMed: 20392965]
5. Cao DY, Bai G, Ji Y, Traub RJ. Epigenetic upregulation of metabotropic glutamate receptor 2 in the spinal cord attenuates oestrogen-induced visceral hypersensitivity. *Gut*. 64:1913–1920, 2015 [PubMed: 25378524]
6. Cao Y, Xie QF, Li K, Light AR, Fu KY. Experimental occlusal interference induces long-term masticatory muscle hyperalgesia in rats. *Pain*. 144:287–293, 2009 [PubMed: 19473767]
7. Chaplan SR, Bach FW, Pogrel JW, Chung JM, Yaksh TL. Quantitative assessment of tactile allodynia in the rat paw. *J Neurosci Methods*. 53:55–63, 1994 [PubMed: 7990513]
8. Chen Q, Heinricher MM. Descending Control Mechanisms and Chronic Pain. *Curr Rheumatol Rep*. 21:13, 2019 [PubMed: 30830471]
9. Cortelli P, Pierangeli G. Chronic pain-autonomic interactions. *Neurol Sci*. 24 Suppl 2:S68–70, 2003 [PubMed: 12811596]
10. Danilo VN, Filippo V, Emanuele C, Francesco I, Laura L, Di MB, Elizaveta K. Innovative regenerative medicine in the management of knee OA: The role of Autologous Protein Solution. *J Clin Orthop Traum*. 10:49–52, 2019
11. Denk F, Crow M, Didangelos A, Lopes DM, McMahon SB. Persistent Alterations in Microglial Enhancers in a Model of Chronic Pain. *Cell Rep*. 15:1771–1781, 2016 [PubMed: 27184839]
12. Dinarello CA, Novick D, Rubinstein M, Lonnemann G. Interleukin 18 and interleukin 18 binding protein: possible role in immunosuppression of chronic renal failure. *Blood Purif*. 21:258–270, 2003 [PubMed: 12784053]
13. Donnelly CR, Andriessen AS, Chen G, Wang K, Jiang C, Maixner W, Ji RR. Central Nervous System Targets: Glial Cell Mechanisms in Chronic Pain. *Neurotherapeutics*. 17:846–860, 2020 [PubMed: 32820378]

14. Duan LL, Qiu XY, Wei SQ, Su HY, Bai FR, Traub RJ, Zhou Q, Cao DY. Spinal CCK contributes to somatic hyperalgesia induced by orofacial inflammation combined with stress in adult female rats. *Eur J Pharmacol.* 913:174619, 2021 [PubMed: 34748768]
15. Foldy C, Lee SY, Szabadics J, Neu A, Soltesz I. Cell type-specific gating of perisomatic inhibition by cholecystokinin. *Nat Neurosci.* 10:1128–1130, 2007 [PubMed: 17676058]
16. Gao YJ, Ji RR. Targeting astrocyte signaling for chronic pain. *Neurotherapeutics.* 7:482–493, 2010 [PubMed: 20880510]
17. Gong QY, Lin Y, Lu ZN, Xiao ZM. Microglia-Astrocyte Cross Talk through IL-18/IL-18R Signaling Modulates Migraine-like Behavior in Experimental Models of Migraine. *Neuroscience.* 451:207–215, 2020 [PubMed: 33137409]
18. Guo W, Miyoshi K, Dubner R, Gu M, Li M, Liu J, Yang J, Zou S, Ren K, Noguchi K, Wei F. Spinal 5-HT<sub>3</sub> receptors mediate descending facilitation and contribute to behavioral hypersensitivity via a reciprocal neuron-glial signaling cascade. *Mol Pain.* 10:35, 2014 [PubMed: 24913307]
19. Guo W, Wang H, Zou S, Wei F, Dubner R, Ren K. Long lasting pain hypersensitivity following ligation of the tendon of the masseter muscle in rats: A model of myogenic orofacial pain. *Mol Pain.* 6:40, 2010 [PubMed: 20633279]
20. Gwilym SE, Filippini N, Douaud G, Carr AJ, Tracey I. Thalamic Atrophy Associated With Painful Osteoarthritis of the Hip Is Reversible After Arthroplasty A Longitudinal Voxel-Based Morphometric Study. *Arthritis Rheum.* 62:2930–2940, 2010 [PubMed: 20518076]
21. Gwilym SE, Keltner JR, Warnaby CE, Carr AJ, Chizh B, Chessell I, Tracey I. Psychophysical and functional imaging evidence supporting the presence of central sensitization in a cohort of osteoarthritis patients. *Arthritis Rheum.* 61:1226–1234, 2009 [PubMed: 19714588]
22. Hao L, Wen D, Gou H, Yu F, Cong B, Ma C. Over-expression of CCK1 Receptor Reverse Morphine Dependence. *Int J Pept Res Ther.* 24:471–477, 2018 [PubMed: 30147637]
23. Hargreaves K, Dubner R, Brown F, Flores C, Joris J. A new and sensitive method for measuring thermal nociception in cutaneous hyperalgesia. *Pain.* 32:77–88, 1988 [PubMed: 3340425]
24. Heinricher MM, Neubert MJ. Neural basis for the hyperalgesic action of cholecystokinin in the rostral ventromedial medulla. *J Neurophysiol.* 92:1982–1989, 2004 [PubMed: 15152023]
25. Henderson SE, Tudares MA, Tashman S, Almarza AJ. Decreased Temporomandibular Joint Range of Motion in a Model of Early Osteoarthritis in the Rabbit. *J Oral Maxil Surg.* 73:1695–1705, 2015
26. Hylden JL, Wilcox GL. Intrathecal morphine in mice: a new technique. *Eur J Pharmacol.* 67:313–316, 1980 [PubMed: 6893963]
27. Ji RR, Nackley A, Huh Y, Terrando N, Maixner W. Neuroinflammation and Central Sensitization in Chronic and Widespread Pain. *Anesthesiology.* 129:343–366, 2018 [PubMed: 29462012]
28. Jiang M, Bo JH, Lei YS, Hu F, Xia ZR, Liu Y, Lu CE, Sun YE, Hou BL, Ni K, Ma ZL, Gu XP. Anxiety-induced hyperalgesia in female rats is mediated by cholecystokinin 2 receptor in rostral ventromedial medulla and spinal 5-hydroxytryptamine 2B receptor. *JPain Res.* 12:2009–2026, 2019 [PubMed: 31308730]
29. Jiao K, Wang MQ, Niu LN, Dai J, Yu SB, Liu XD, Wang GW. Death and proliferation of chondrocytes in the degraded mandibular condylar cartilage of rats induced by experimentally created disordered occlusion. *Apoptosis.* 14(1):22–30, 2009 [PubMed: 19052875]
30. Chen Jinwu, Jun Zhang, Zhao Yimin, Yuan Lintian, Nie Xin. Hyperalgesia in response to traumatic occlusion and GFAP expression in rat parabrachial nucleus: modulation with fluorocitrate. *Cell Tissue Res.* 329(2):231–7, 2007 [PubMed: 17443351]
31. Kanno T, Nagata T, Yamamoto S, Okamura H, Nishizaki T. Interleukin-18 stimulates synaptically released glutamate and enhances postsynaptic AMPA receptor responses in the CA1 region of mouse hippocampal slices. *Brain Res.* 1012:190–193, 2004 [PubMed: 15158178]
32. Kosek E, Ordeberg G. Abnormalities of somatosensory perception in patients with painful osteoarthritis normalize following successful treatment. *Eur J Pain.* 4:229–238, 2000 [PubMed: 10985866]

33. Kotiranta U, Forssell H, Kauppila T. Painful temporomandibular disorders (TMD) and comorbidities in primary care: associations with pain-related disability. *Acta Odontol Scand.* 77:22–27, 2019 [PubMed: 30264645]
34. Lee S, Soltesz I. Requirement for CB1 but not GABAB receptors in the cholecystokinin mediated inhibition of GABA release from cholecystokinin expressing basket cells. *J Physiol.* 589, 2011
35. Lee SY, Foldy C, Szabadics J, Soltesz I. Cell-type-specific CCK2 receptor signaling underlies the cholecystokinin-mediated selective excitation of hippocampal parvalbumin-positive fast-spiking basket cells. *J Neurosci.* 31:10993–11002, 2011 [PubMed: 21795548]
36. Li JH, Yang JL, Wei SQ, Li ZL, Collins AA, Zou M, Wei F, Cao DY. Contribution of central sensitization to stress-induced spreading hyperalgesia in rats with orofacial inflammation. *Mol Brain.* 13:106, 2020 [PubMed: 32723345]
37. Lin L, Huang M, Lan M, Jing L. Different role of cholecystokinin (CCK)-A and CCK-B receptors in relapse to morphine dependence in rats. *Behav Brain Res.* 120:105–110, 2001 [PubMed: 11173090]
38. Liu S, Liu YP, Lv Y, Yao JL, Yue DM, Zhang MY, Qi DY, Liu GJ. IL-18 Contributes to Bone Cancer Pain by Regulating Glia Cells and Neuron Interaction. *J Pain.* 19:186–195, 2018 [PubMed: 29079540]
39. Liu X, Wang G, Ai G, Xu X, Niu X, Zhang M. Selective Ablation of Descending Serotonin from the Rostral Ventromedial Medulla Unmasks Its Pro-Nociceptive Role in Chemotherapy-Induced Painful Neuropathy. *J Pain Res.* 13:3081–3094, 2020 [PubMed: 33262643]
40. Liu X, Zhou KX, Yin NN, Zhang CK, Shi MH, Zhang HY, Wang DM, Xu ZJ, Zhang JD, Li JL, Wang MQ. Malocclusion Generates Anxiety-Like Behavior Through a Putative Lateral Habenula-Mesencephalic Trigeminal Nucleus Pathway. *Front Mol Neurosci.* 12:174, 2019 [PubMed: 31427925]
41. Liu X, Zhou KX, Yin NN, Zhang CK, Shi MH, Zhang HY, Wang DM, Xu ZJ, Zhang JD, Li JL, Wang MQ. Malocclusion Generates Anxiety-Like Behavior Through a Putative Lateral Habenula-Mesencephalic Trigeminal Nucleus Pathway. *Front Mol Neurosci.* 12:174, 2019 [PubMed: 31427925]
42. Liu ZY, Song ZW, Guo SW, He JS, Wang SY, Zhu JG, Yang HL, Liu JB. CXCL12/CXCR4 signaling contributes to neuropathic pain via central sensitization mechanisms in a rat spinal nerve ligation model. *CNS Neurosci Ther.* 25:922–936, 2019 [PubMed: 30955244]
43. Lovick TA. Pro-nociceptive action of cholecystokinin in the periaqueductal grey: a role in neuropathic and anxiety-induced hyperalgesic states. *Neurosci Biobehav Rev.* 32:852–862, 2008 [PubMed: 18295886]
44. Matsuka Y, Afroz S, Dalanon JC, Iwasa T, Waskitho A, Oshima M. The role of chemical transmitters in neuron-glia interaction and pain in sensory ganglion. *Neurosci Biobehav Rev.* 108:393–399, 2020 [PubMed: 31785264]
45. Miyoshi K, Obata K, Kondo T, Okamura H, Noguchi K. Interleukin-18-mediated microglia/astrocyte interaction in the spinal cord enhances neuropathic pain processing after nerve injury. *J Neurosci.* 28:12775–12787, 2008 [PubMed: 19036970]
46. Moayed M, Hodaie M. Trigeminal nerve and white matter brain abnormalities in chronic orofacial pain disorders. *Pain Rep.* 4:e755, 2019 [PubMed: 31579849]
47. Mokhtar M, Singh P: Neuroanatomy, Periaqueductal Gray. In: StatPearls, Treasure Island (FL), 2021.
48. Moreno-Fernandez AM, Jimenez-Castellanos E, Iglesias-Linares A, Bueso-Madrid D, Fernandez-Rodriguez A, de Miguel M. Fibromyalgia syndrome and temporomandibular disorders with muscular pain. A review. *Mod Rheumatol.* 27:210–216, 2017 [PubMed: 27539739]
49. Moser B, Hochreiter B, Herbst R, Schmid JA. Fluorescence colocalization microscopy analysis can be improved by combining object-recognition with pixel-intensity-correlation. *Biotechnol J.* 12, 2017
50. Nam Y, Kim JH, Kim JH, Jha MK, Jung JY, Lee MG, Choi IS, Jang IS, Lim DG, Hwang SH, Cho HJ, Suk K. Reversible Induction of Pain Hypersensitivity following Optogenetic Stimulation of Spinal Astrocytes. *Cell Rep.* 17:3049–3061, 2016 [PubMed: 27974216]

51. Nicholas M, Vlaeyen JWS, Rief W, Barke A, Aziz Q, Benoliel R, Cohen M, Evers S, Giamberardino MA, Goebel A, Korwisi B, Perrot S, Svensson P, Wang SJ, Treede RD, Pain ITfCoC. The IASP classification of chronic pain for ICD-11: chronic primary pain. *Pain*. 160:28–37, 2019 [PubMed: 30586068]
52. Nieto FR, Clark AK, Grist J, Hathway GJ, Chapman V, Malcangio M. Neuron-immune mechanisms contribute to pain in early stages of arthritis. *J Neuroinflammation*. 13:96, 2016 [PubMed: 27130316]
53. O'Brien CE, Bonanno L, Zhang H, Wyss-Coray T. Beclin 1 regulates neuronal transforming growth factor-beta signaling by mediating recycling of the type I receptor ALK5. *Mol Neurodegener*. 10:69, 2015 [PubMed: 26692002]
54. Old EA, Clark AK, Malcangio M. The role of glia in the spinal cord in neuropathic and inflammatory pain. *Handb Exp Pharmacol*. 227:145–170, 2015 [PubMed: 25846618]
55. Ossipov MH, Lai J, Malan TP, Porreca F. Spinal and supraspinal mechanisms of neuropathic pain. *Ann N Y Acad Sci*. 909:12–24, 2000 [PubMed: 10911921]
56. Peirs C, Williams S, Zhao X, Arokiaraj CM, Ferreira DW, Noh MC, Smith KM, Halder P, Corrigan KA, Gedeon JY. Mechanical Allodynia Circuitry in the Dorsal Horn Is Defined by the Nature of the Injury. *Neuron*. 109(1):73–90.e7, 2021 [PubMed: 33181066]
57. Pilat D, Piotrowska A, Rojewska E, Jurga A, Slusarczyk J, Makuch W, Basta-Kaim A, Przewlocka B, Mika J. Blockade of IL-18 signaling diminished neuropathic pain and enhanced the efficacy of morphine and buprenorphine. *Mol Cell Neurosci*. 71:114–124, 2016 [PubMed: 26763728]
58. Potter RM, Harikumar KG, Wu SV, Miller LJ. Differential sensitivity of types 1 and 2 cholecystokinin receptors to membrane cholesterol. *J Lipid Res*. 53:137–148, 2012 [PubMed: 22021636]
59. Ren K An improved method for assessing mechanical allodynia in the rat. *Physiol Behav*. 67:711–716, 1999 [PubMed: 10604842]
60. Ren K, Dubner R. Interactions between the immune and nervous systems in pain. *Nature Medicine*. 16:1267–1276, 2010
61. Rex DAB, Agarwal N, Prasad TSK, Kandasamy RK, Subbannayya Y, Pinto SM. A comprehensive pathway map of IL-18-mediated signalling. *J Cell Commun Signal*. 14:257–266, 2020 [PubMed: 31863285]
62. Roca-Lapirot O, Fossat P, Ma S, Egron K, Trigilio G, Lopez-Gonzalez MJ, Covita J, Bouali-Benazzouz R, Favereaux A, Gundlach AL, Landry M. Acquisition of analgesic properties by the cholecystokinin (CCK)/CCK2 receptor system within the amygdala in a persistent inflammatory pain condition. *Pain*. 160:345–357, 2019 [PubMed: 30281531]
63. Salter MW, Beggs S. Sublime microglia: expanding roles for the guardians of the CNS. *Cell*. 158:15–24, 2014 [PubMed: 24995975]
64. Scholz J, Woolf CJ. The neuropathic pain triad: neurons, immune cells and glia. *Nat Neurosci*. 10:1361–1368, 2007 [PubMed: 17965656]
65. Schomberg D, Olson JK. Immune responses of microglia in the spinal cord: contribution to pain states. *Exp Neurol*. 234:262–270, 2012 [PubMed: 22226600]
66. Shavit Y, Wolf G, Goshen I, Livshits D, Yirmiya R. Interleukin-1 antagonizes morphine analgesia and underlies morphine tolerance. *Pain*. 115:50–59, 2005 [PubMed: 15836969]
67. Staud R. Evidence of involvement of central neural mechanisms in generating fibromyalgia pain. *Curr Rheumatol Rep*. 4:299–305, 2002 [PubMed: 12126581]
68. Staud R. Abnormal pain modulation in patients with spatially distributed chronic pain: fibromyalgia. *Rheum Dis Clin North Am*. 35:263–274, 2009 [PubMed: 19647141]
69. Staud R. Evidence for Shared Pain Mechanisms in Osteoarthritis, Low Back Pain, and Fibromyalgia. *Curr Rheumat Rep*. 13:513–520, 2011
70. Sugiyo S, Takemura M, Dubner R, Ren K. Trigeminal transition zone/rostral ventromedial medulla connections and facilitation of orofacial hyperalgesia after masseter inflammation in rats. *J Comp Neurol*. 493:510–523, 2005 [PubMed: 16304628]
71. Thamsermsang O, Akarasereenont P, Laohapand T, Panich U. IL-1beta-induced modulation of gene expression profile in human dermal fibroblasts: the effects of Thai herbal Sahatsatara



- formula, piperine and gallic acid possessing antioxidant properties. *BMC Complement Altern Med.* 17:32, 2017 [PubMed: 28068976]
72. Treede RD, Rief W, Barke A, Aziz Q, Bennett MI, Benoliel R, Cohen M, Evers S, Finnerup NB, First MB, Giamberardino MA, Kaasa S, Korwisi B, Kosek E, Lavand'homme P, Nicholas M, Perrot S, Scholz J, Schug S, Smith BH, Svensson P, Vlaeyen JWS, Wang SJ. Chronic pain as a symptom or a disease: the IASP Classification of Chronic Pain for the International Classification of Diseases (ICD-11). *Pain.* 160:19–27, 2019 [PubMed: 30586067]
  73. Tripathi S, Flobak A, Chawla K, Baudot A, Bruland T, Thommesen L, Kuiper M, Laegreid A. The gastrin and cholecystokinin receptors mediated signaling network: a scaffold for data analysis and new hypotheses on regulatory mechanisms. *BMC Syst Biol.* 9:40, 2015 [PubMed: 26205660]
  74. Turp JC, Schindler H. The dental occlusion as a suspected cause for TMDs: epidemiological and etiological considerations. *J Oral Rehabil.* 39:502–512, 2012 [PubMed: 22486535]
  75. Vanderwall AG, Milligan ED. Cytokines in Pain: Harnessing Endogenous Anti-Inflammatory Signaling for Improved Pain Management. *Front Immunol.* 10:3009, 2019 [PubMed: 31921220]
  76. Wang YL, Zhang J, Zhang M, Lu L, Wang X, Guo M, Zhang X, Wang MQ. Cartilage degradation in temporomandibular joint induced by unilateral anterior crossbite prosthesis. *Oral Diseases.* 20:301–306, 2014 [PubMed: 23614573]
  77. Wu YY, Kadota-Watanabe C, Ogawa T, Moriyama K. Combination of estrogen deficiency and excessive mechanical stress aggravates temporomandibular joint osteoarthritis in vivo. *Arch Oral Biol.* 102:39–46, 2019 [PubMed: 30959278]
  78. Xie JY, Herman DS, Stiller CO, Gardell LR, Ossipov MH, Lai J, Porreca F, Vanderah TW. Cholecystokinin in the rostral ventromedial medulla mediates opioid-induced hyperalgesia and antinociceptive tolerance. *J Neurosci.* 25:409–416, 2005 [PubMed: 15647484]
  79. Xin Z, Hartung JE, Bortsov AV, Seungtae K, O'Buckley SC, Julia K, Nackley AG. Sustained stimulation of  $\beta$ 2- and  $\beta$ 3-adrenergic receptors leads to persistent functional pain and neuroinflammation. *Brain Behav Immun.* 73:520–532, 2018 [PubMed: 29935309]
  80. Xue Y, Wei SQ, Wang PX, Wang WY, Liu EQ, Traub RJ, Cao DY. Down-regulation of Spinal 5-HT2A and 5-HT2C Receptors Contributes to Somatic Hyperalgesia induced by Orofacial Inflammation Combined with Stress. *Neuroscience.* 440, 2020
  81. Yamamoto T, Nozaki-Taguchi N. Role of cholecystokinin-B receptor in the maintenance of thermal hyperalgesia induced by unilateral constriction injury to the sciatic nerve in the rat. *Neurosci Lett.* 202:89–92, 1995 [PubMed: 8787838]
  82. Yamamoto T, Nozaki-Taguchi N. The Effects of Intrathecally Administered FK480, a Cholecystokinin-A Receptor Antagonist, and YM022, a Cholecystokinin-B Receptor Antagonist, on the Formalin Test in the Rat. *Anesth Analg.* 83:107, 1996 [PubMed: 8659718]
  83. Yang Y, Li H, Li TT, Luo H, Gu XY, Lu N, Ji RR, Zhang YQ. Delayed activation of spinal microglia contributes to the maintenance of bone cancer pain in female Wistar rats via P2X7 receptor and IL-18. *J Neurosci.* 35:7950–7963, 2015 [PubMed: 25995479]
  84. Ying YL, Wei XH, Xu XB, She SZ, Zhou LJ, Lv J, Li D, Zheng B, Liu XG. Over-expression of P2X7 receptors in spinal glial cells contributes to the development of chronic postsurgical pain induced by skin/muscle incision and retraction (SMIR) in rats. *Exp Neurol.* 261:836–843, 2014 [PubMed: 25242211]
  85. Zhang HY, Xie MJ, Yang HX, Liu X, Ren HT, Zhang M, Lu L, Liu XD, Zhang J, Wang MQ. Catabolic changes of rat temporomandibular joint discs induced by unilateral anterior crossbite. *J Oral Rehabil.* 46:340–348, 2019 [PubMed: 30556174]
  86. Zhang M, Wang H, Zhang J, Zhang H, Yang H, Wan X, Jing L, Lu L, Liu X, Yu S. Unilateral anterior crossbite induces aberrant mineral deposition in degenerative temporomandibular cartilage in rats. *Osteoarthritis Cartilage.* 24:921–931, 2016 [PubMed: 26746151]
  87. Zhang W, Shannon G, Zhang D, Xie JY, Agnes RS, Hamid B, Hrubby VJ, Naomi R, Ossipov MH, Vanderah TW. Neuropathic pain is maintained by brainstem neurons co-expressing opioid and cholecystokinin receptors. *Brain.* 132:778–787, 2009 [PubMed: 19050032]
  88. Zhang ZJ, Jiang BC, Gao YJ. Chemokines in neuron-glial cell interaction and pathogenesis of neuropathic pain. *Cell Mol Life Sci.* 74:3275–3291, 2017 [PubMed: 28389721]

89. Zúiga-Herrera ID, Herrera-Atoche JR, Escoffié-Ramírez M, Casanova-Rosado JF, Alonzo-Echeverría ML, Aguilar-Pérez FJ. Malocclusion complexity as an associated factor for temporomandibular disorders. A case-control study. *Cranio*. 7;1–6, 2021

Author Manuscript

Author Manuscript

Author Manuscript

Author Manuscript

### Highlights

- Malocclusion induces widespread somatic pain hypersensitivity, a typical characteristic of FMS.
- CCK-dependent descending facilitation contributes to the development of TMD and FMS comorbidity.
- IL-18 in the spinal cord is important for the development of somatic pain hypersensitivity.
- CCK/IL-18-mediated neuronal and glial cascades are involved in the somatic pain hypersensitivity.

**Perspective:**

CCK1 receptor-dependent descending facilitation may mediate central mechanisms underlying the development of widespread somatic pain via a reciprocal neuron-glia signaling cascade, providing novel therapeutic targets for the clinical treatment of TMD and FMS comorbidities.

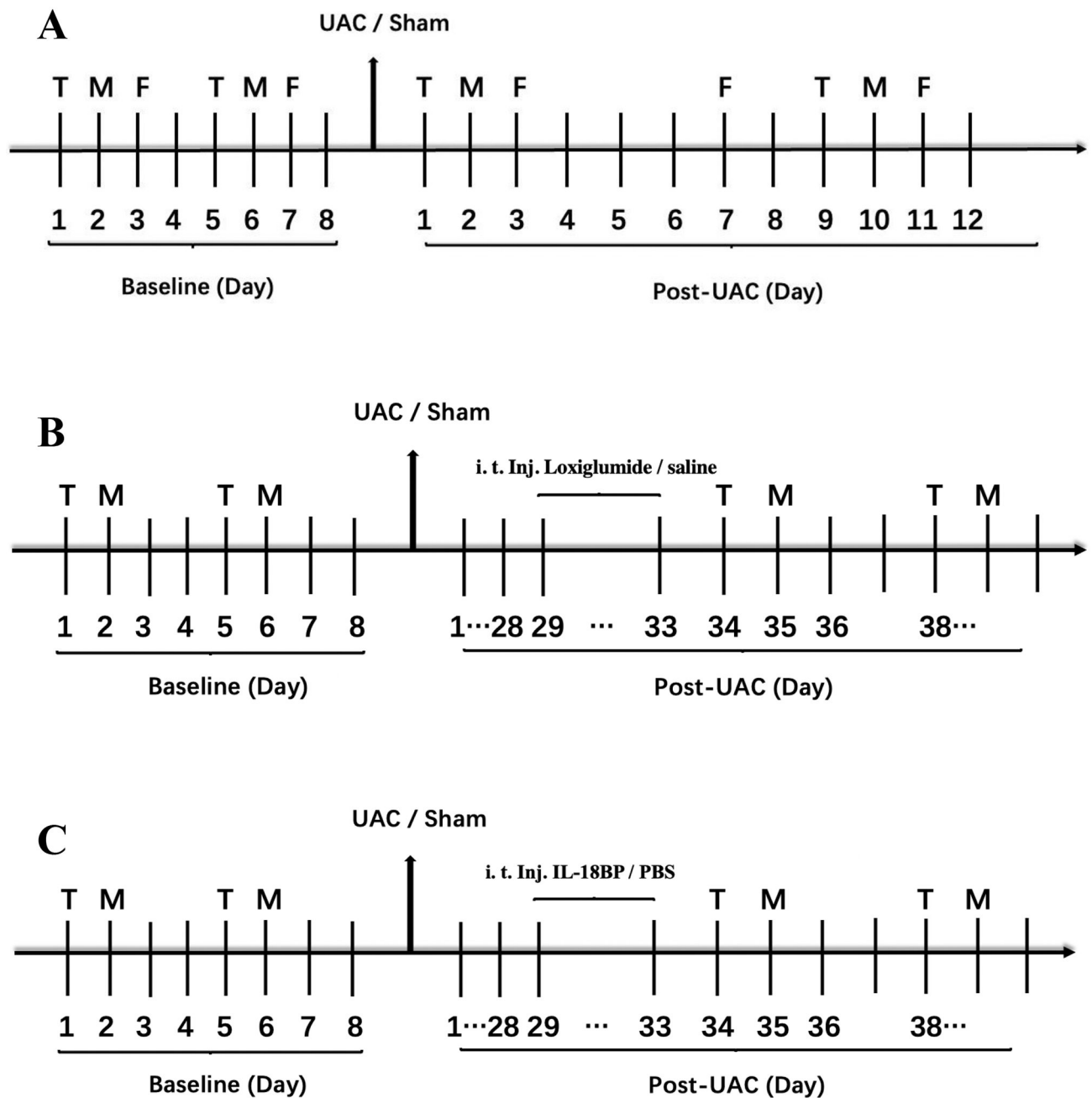


**Figure 1.**

Experimental design. A. The baselines of the thermal withdrawal latency (T), mechanical withdrawal threshold (M) and maxillofacial mechanical threshold (F) were tested before UAC. From the first day after UAC was established, the thermal withdrawal latency and mechanical withdrawal threshold were measured on the first and second days and then every 8 days. On day 3 after UAC was established, the maxillofacial mechanical threshold was tested, and then every 4 days. The measurement continued until the pain threshold returned to the baseline level. UAC, unilateral anterior crossbite. CCK1 receptor antagonist

loxiglumide (B) or IL-18-binding protein (IL-18BP) (C) was intrathecally injected for 5 consecutive days at 4 weeks post UAC.

Author Manuscript

Author Manuscript

Author Manuscript

Author Manuscript

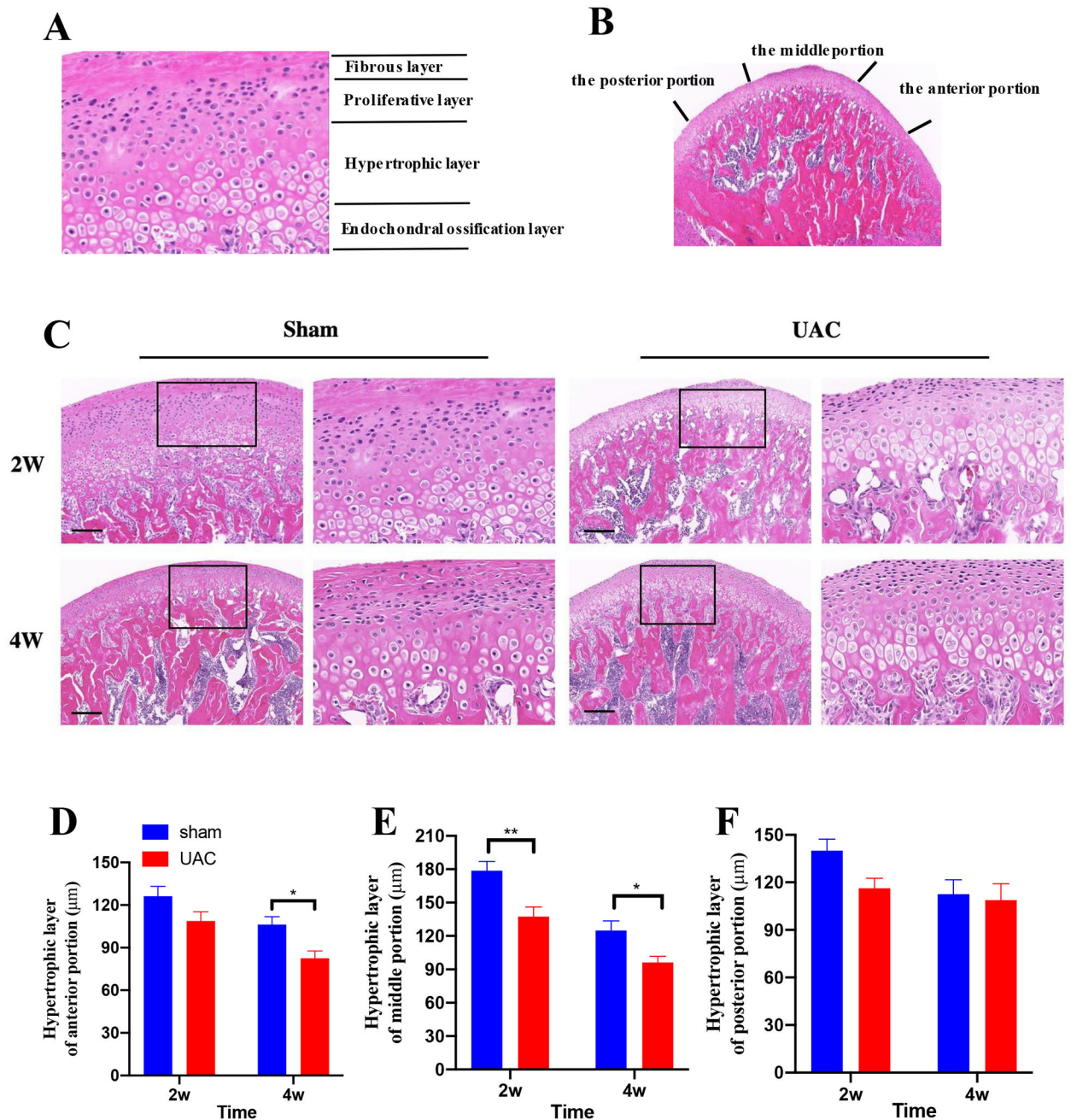


**Figure 2.**

The pathological changes in the condyle cartilage. A: The condyle cartilage includes four layers: the fibrous layer, the proliferative layer, the hypertrophic layer and the endochondral ossification layer. B: Delineation of the anterior, middle and posterior portion of the condyle cartilage. C: Example of condyle cartilage from sham and 2, 4 weeks post UAC, Bar = 200  $\mu\text{m}$ . The boxes depict the regions of higher magnification in each section. The thickness of hypertrophic layer of anterior portion (D), middle portion (E) and posterior portion (F). \*, \*\* $p < 0.05, 0.01$  vs. the sham group.

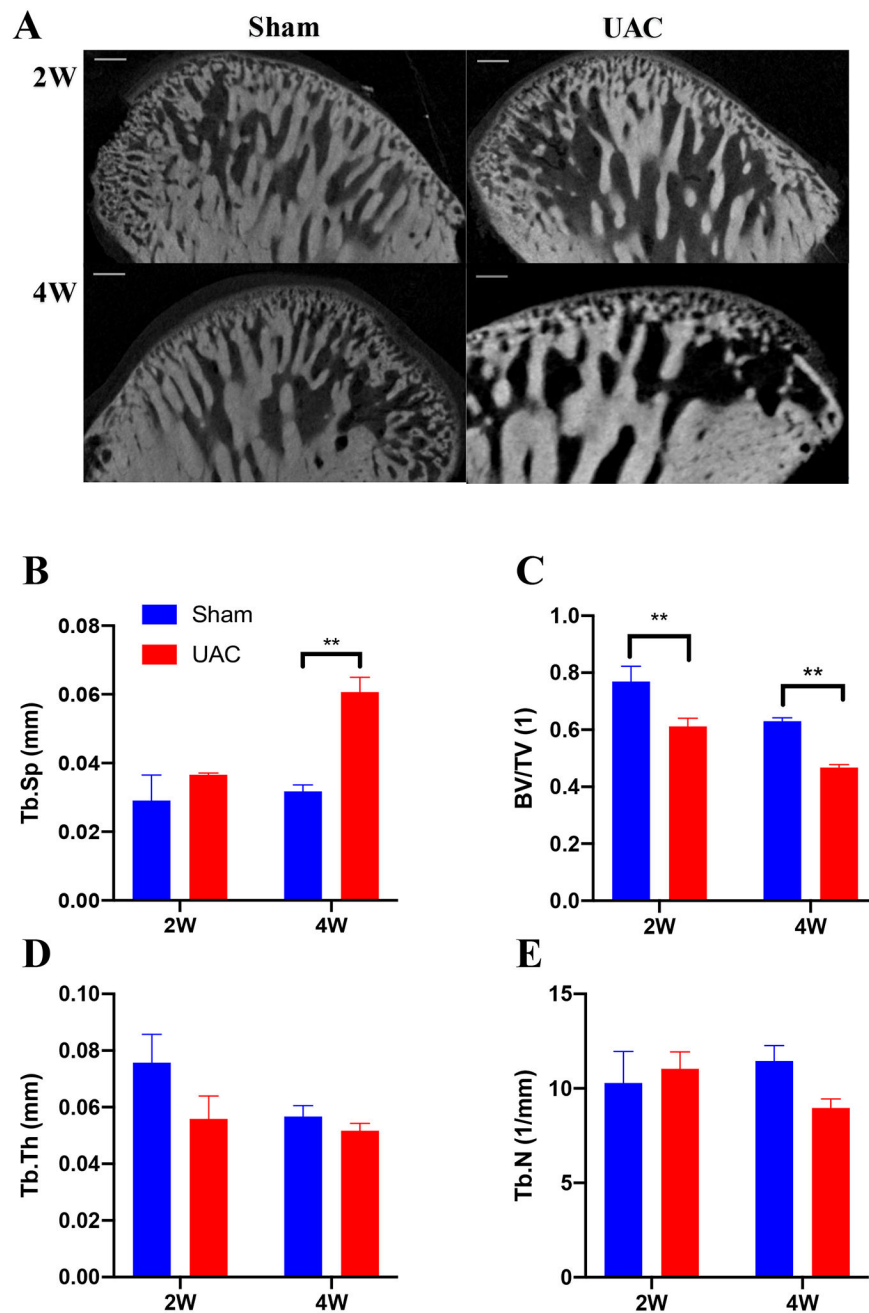


**Figure 3.**

The micro-computed tomography images and bone histomorphology parameters of temporomandibular joint condyles. A: The micro-computed tomography images reflect the changes in the subchondral bone morphology of the condyle in three dimensions at 2 and 4 weeks post UAC, respectively. Bar = 160  $\mu$ m. B: The trabecular bone separation (Tb. Sp). C: Bone volume/total volume (BV/TV). D: Trabecular thickness (Tb. Th). E: Number of trabeculae (Tb. N). \*\*  $p < 0.01$  vs. sham.



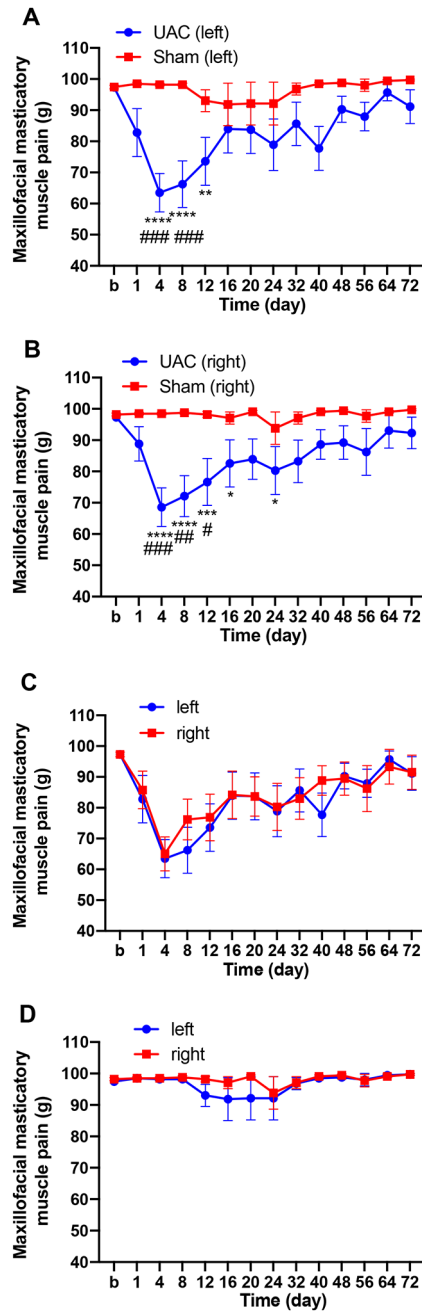


**Figure 4.** UAC reduced maxillofacial mechanical threshold in female rats. A, B: Maxillofacial mechanical threshold ipsilateral (A) and contralateral (B) in the UAC and sham treated rats (n = 9–11 per group). \*, \*\*, \*\*\*  $p < 0.05, 0.01, 0.001$  vs. baseline (b); #, ##, ###  $p < 0.05, 0.01, 0.001$  vs. the sham group at the same time point. C, D: There were no differences in the maxillofacial mechanical threshold between the left and right sides in the UAC group (C) and sham group (D).

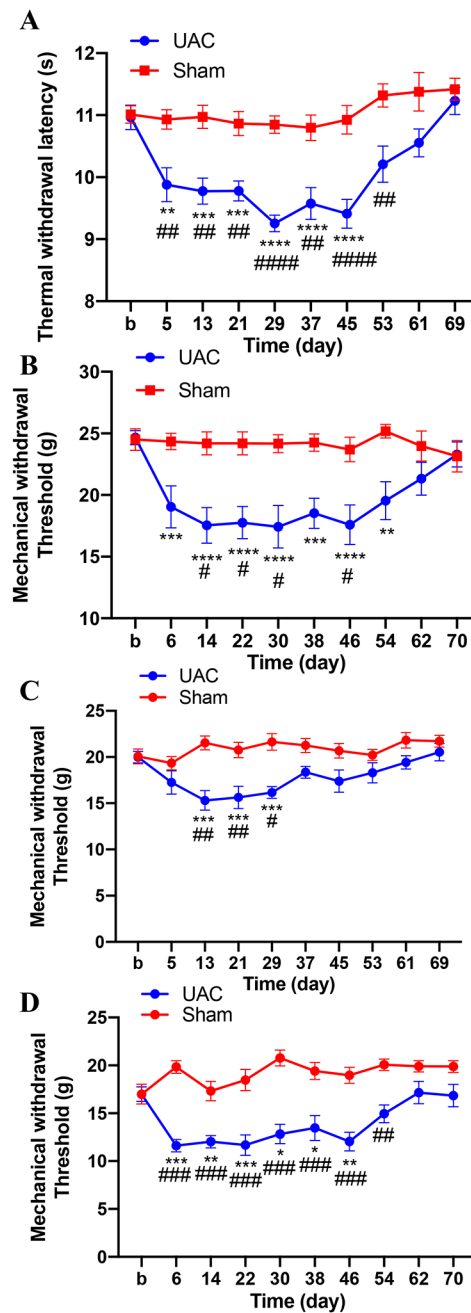


**Figure 5.**

Thermal hyperalgesia in the hind paws and mechanical allodynia in the hind paws, the upper back and thigh of rats induced by UAC. A: Hindpaw thermal withdrawal latency in UAC and sham-treated rats ( $n = 11$  per group). B: Hindpaw mechanical withdrawal threshold ( $n = 11$ ). C: Upper back mechanical withdrawal threshold ( $n = 10$ ). D: Thigh mechanical withdrawal threshold ( $n = 10$ ). No mechanical allodynia was observed in rats with sham treatment. \*, \*\*, \*\*\*  $p < 0.05, 0.01, 0.001$  vs. baseline, respectively. #, ##, ###  $p < 0.05, 0.01, 0.0001$  vs. the sham group at the same time point.

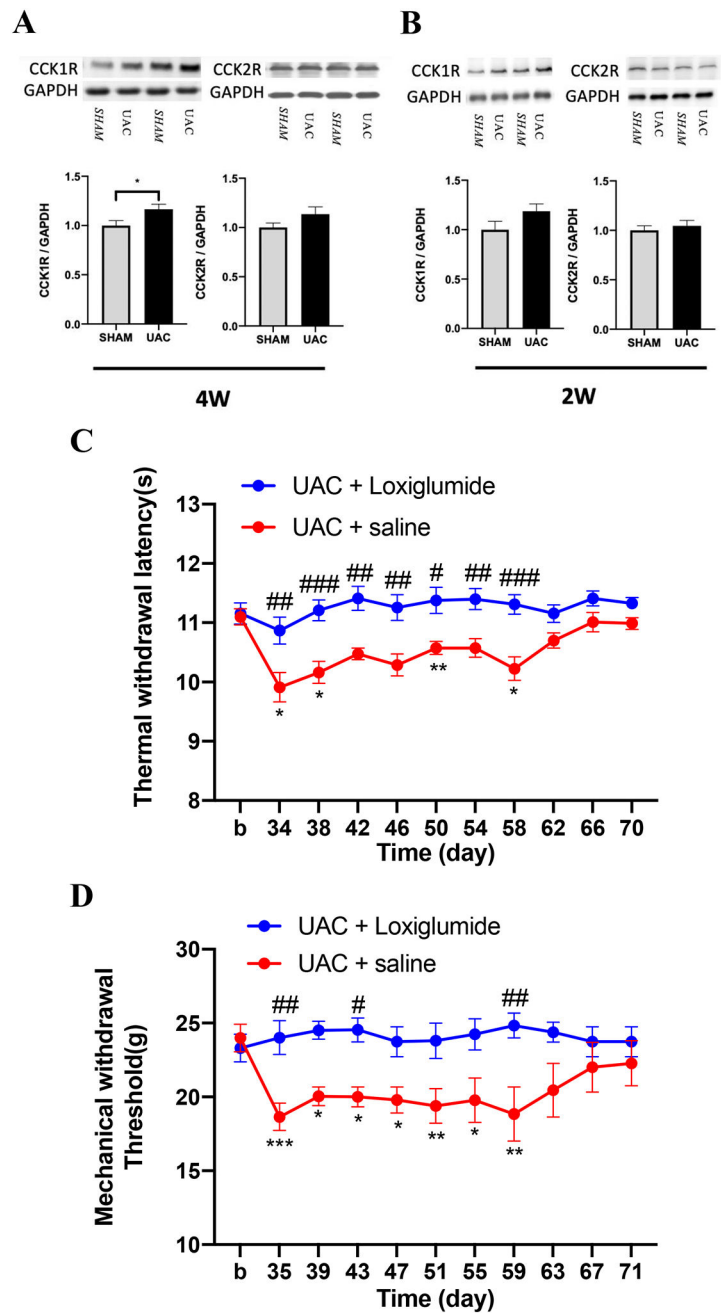


**Figure 6.** CCK1 receptors were involved in the somatic hyperalgesia induced by UAC. A, B: The expression of CCK1 and CCK2 receptors in the L4-L5 spinal dorsal horn at 4 weeks (A) and 2 weeks (B) post UAC, \*  $p < 0.05$  ( $n = 5$  for all groups). C: The CCK1 receptor antagonist loxiglumide ( $n = 9$ ), but not vehicle (saline,  $n = 8$ ), blocked the development of thermal hyperalgesia in female rats. D: Loxiglumide ( $n = 9$ ), but not vehicle ( $n = 8$ ) blocked mechanical allodynia induced by UAC. \*, \*\*, \*\*\*  $p < 0.05, 0.01, 0.001$  vs. baseline (b). #, ##, ###  $p < 0.05, 0.01, 0.001$  vs. the UAC + saline group at the same time point.

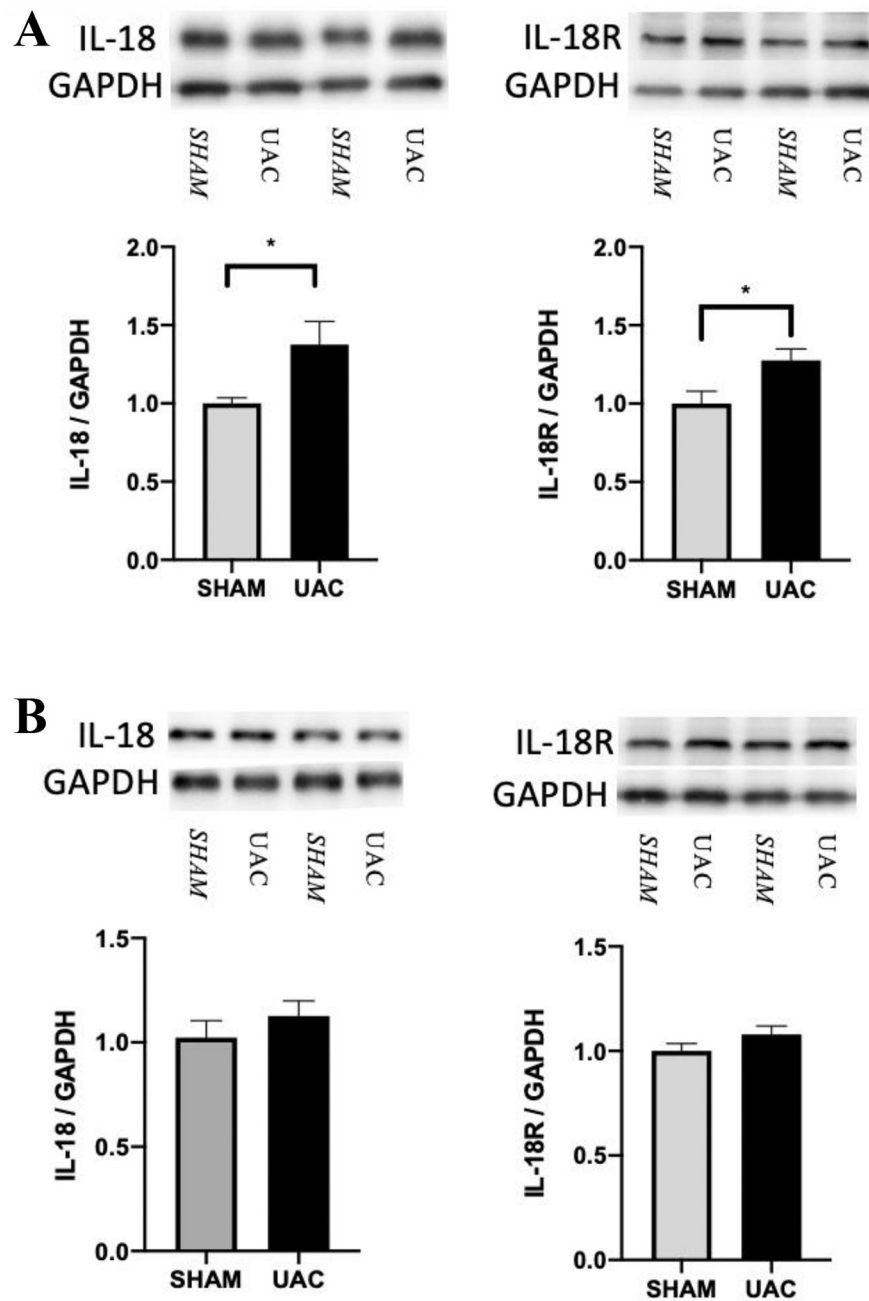


**Figure 7.**

A: The expression of IL-18 and IL-18R in the spinal cord increased at 4 weeks post UAC compared to sham (n = 5 per group). B: The expression of IL-18 and IL-18R at 2 weeks post UAC (n = 5 per group). \*  $p < 0.05$ .

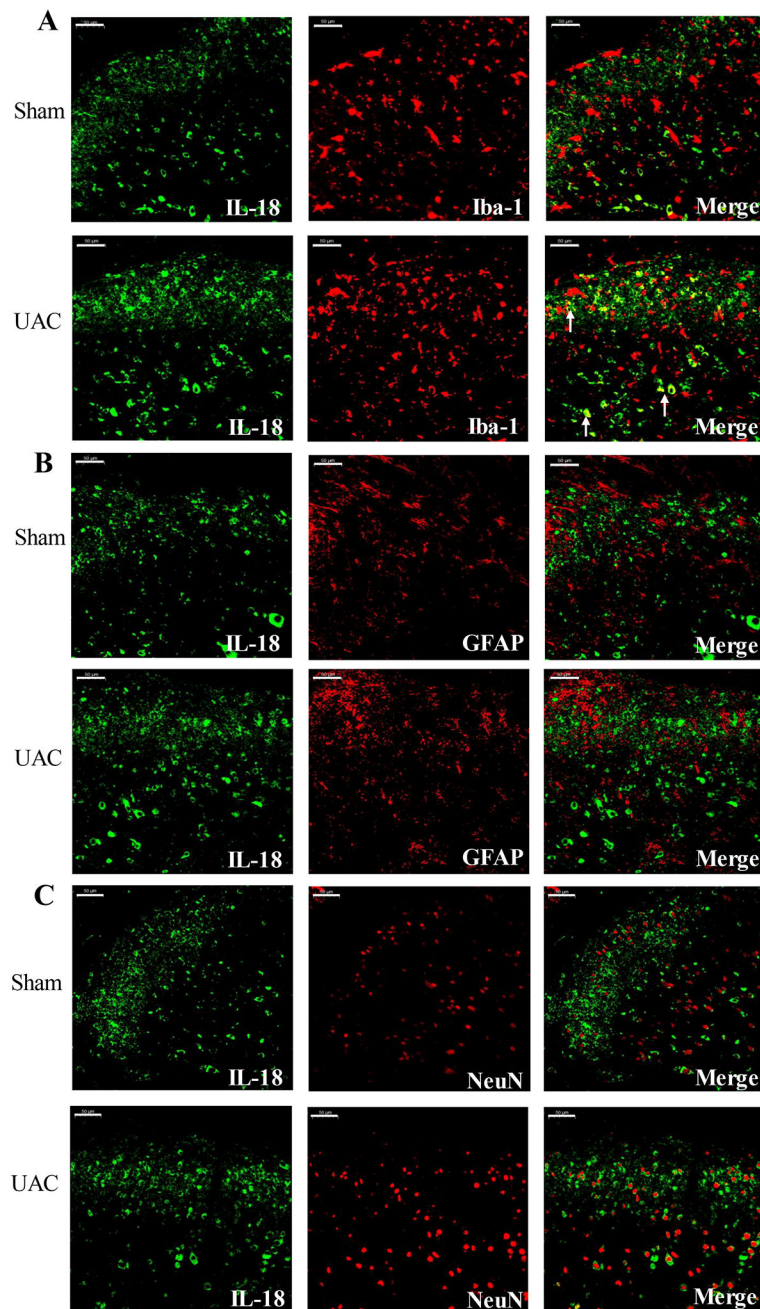


**Figure 8.** IL-18 was co-localized with microglia in the spinal cord post UAC. At 4 weeks post UAC, double immunofluorescence showed that IL-18 (green) was co-localized with Iba-1 (red) (A). IL-18 did not co-localized with GFAP (red) (B) and NeuN (red) (C). Arrows indicate the co-localized cells. Bar = 50  $\mu$ m.

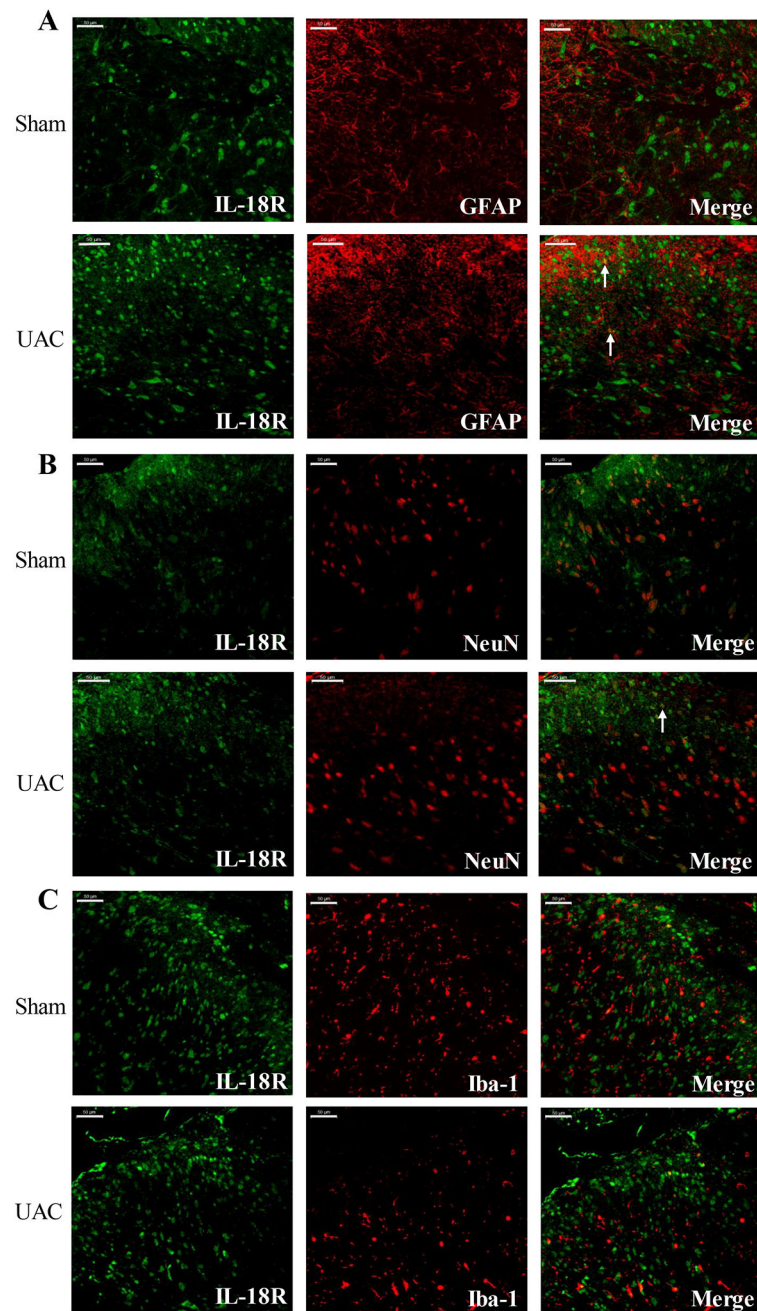


**Figure 9.** IL-18R was co-localized with astrocytes in the spinal cord post UAC, but not with microglia and neurons. Double immunofluorescence showed that IL-18R (green) was co-localized with GFAP (red) (A) and NeuN (red) (B) in the dorsal horn but not with Iba-1 (red) (C) at 4 weeks post UAC. Arrows indicate the co-localized cells. Bar = 50 μm.

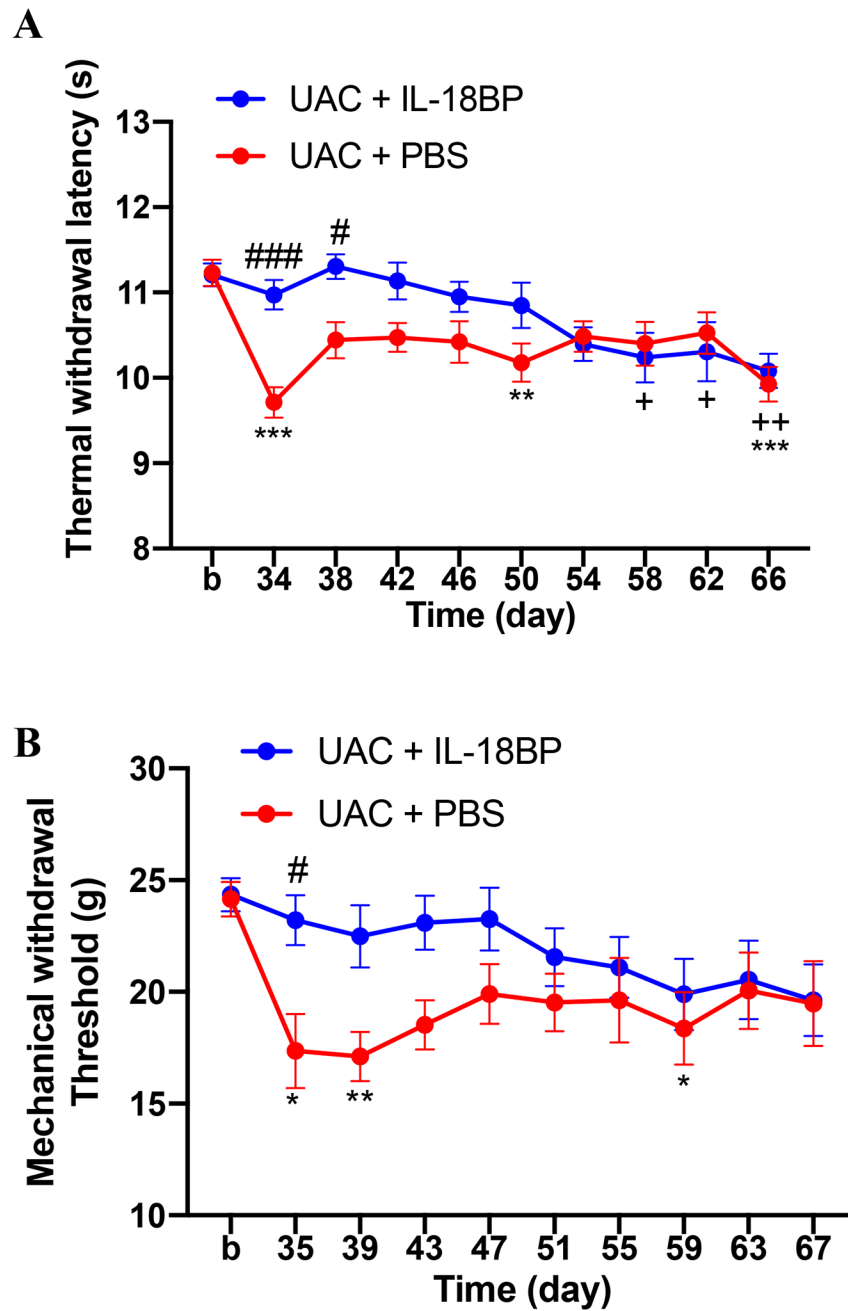


**Figure 10.**

IL-18 receptor antagonist IL-18BP blocked the thermal hyperalgesia (A,  $n = 8$  per group) and mechanical allodynia (B,  $n = 8$  per group) in the hind paws caused by UAC. \*, \*\*, \*\*\*  $p < 0.05, 0.01, 0.001$  vs. baseline (b) (UAC + PBS). +, ++  $p < 0.05, 0.01$  vs. baseline (b) (UAC + IL-18BP). #, ###  $p < 0.05, 0.001$  vs. the UAC + PBS group at the same time point.

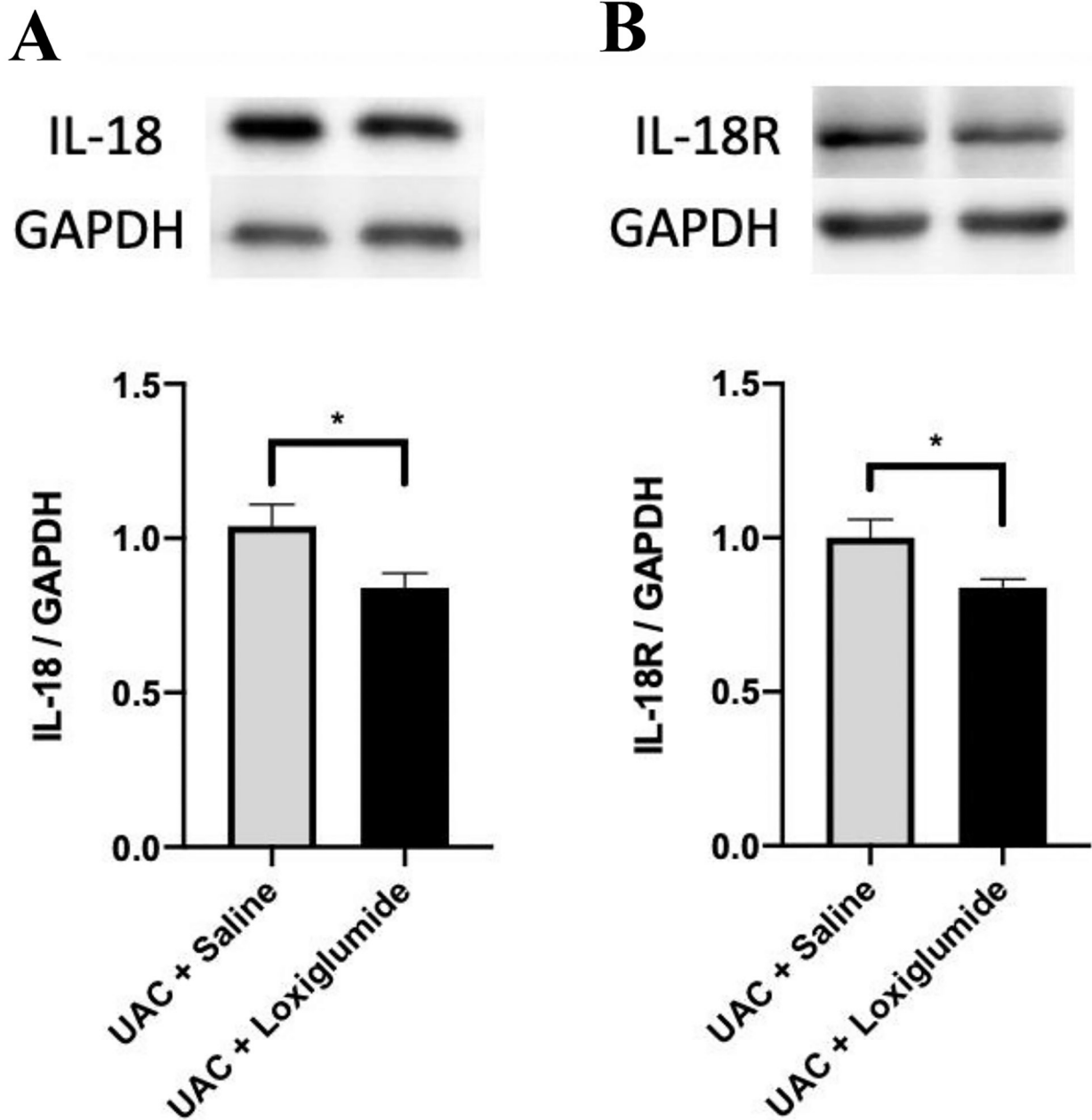


**Figure 11.**

The effect of intrathecal injection of CCK1 receptor antagonist loxiglumide on the expression of IL-18/IL-18R in the L4-L5 spinal cord at 4 weeks post UAC. The expression of IL-18 (A) and IL-18R (B) in the L4-L5 spinal dorsal horn in the UAC + loxiglumide group significantly decreased compared to the UAC + saline group.  $n = 5$  for each group. \*  $p < 0.05$ .